

AD.

12



**CHEMICAL  
SYSTEMS  
LABORATORY**

US Army Armament Research and Development Command  
Aberdeen Proving Ground, Maryland 21010

CONTRACTOR REPORT ARCSL-CR-83062

FUNDAMENTALS OF NON-NEWTONIAN LIQUID FLOW ON SURFACES

by

Simon Rosenblat

Stephen H. Davis

June 1983

CASTAR-INC  
2340 Lawndale Avenue  
Evanston, Illinois 60201

Contract No. DAAK 11-82-C-0078

DTIC  
ELECTRONIC  
DEC 8 1983  
A



REPRODUCED FROM  
BEST AVAILABLE COPY

Approved for public release; distribution unlimited

83 12 08 004

AD-A135543

DTIC FILE COPY

Disclaimer

The findings in this report are not to be construed as an official Department of the Army position unless so designated by other authorizing Documents.

Disposition

Destroy this report when it is no longer needed. Do not return it to the originator.

Unclassified

SECURITY CLASSIFICATION OF THIS PAGE (When Data Entered)

REPORT DOCUMENTATION PAGE		READ INSTRUCTIONS BEFORE COMPLETING FORM
1. REPORT NUMBER ARCSL-CR-83062	2. GOVT ACCESSION NO. <b>A1355713</b>	RECIPIENT'S CATALOG NUMBER
4. TITLE (and Subtitle) Fundamentals of Non-Newtonian Liquid Flow on Surfaces	5. TYPE OF REPORT & PERIOD COVERED Final Report July 1982 - May 1983	
	6. PERFORMING ORG. REPORT NUMBER	
7. AUTHOR(s) Simon Rosenblat Stephen H. Davis	8. CONTRACT OR GRANT NUMBER(s) DAAK 11-82-C-0078	
9. PERFORMING ORGANIZATION NAME AND ADDRESS CASTAR, Inc. 2340 Lawndale Avenue Evanston, IL 60201	10. PROGRAM ELEMENT, PROJECT, TASK AREA & WORK UNIT NUMBERS	
11. CONTROLLING OFFICE NAME AND ADDRESS Commander, Chemical Systems Laboratory ATTN: DRDAR-CLJ-IR Aberdeen Proving Ground, MD 21010	12. REPORT DATE June 1983	
	13. NUMBER OF PAGES 75	
14. MONITORING AGENCY NAME & ADDRESS (if different from Controlling Office) Commander, Chemical Systems Laboratory ATTN: DRDAR-CLB-PO Aberdeen Proving Ground, MD 21010	15. SECURITY CLASS. (of this report) Unclassified	
	15a. DECLASSIFICATION/DOWNGRADING SCHEDULE N A	
16. DISTRIBUTION STATEMENT (of this Report)  Approved for public release; distribution unlimited.		
17. DISTRIBUTION STATEMENT (of the abstract entered in Block 20, if different from Report)		
18. SUPPLEMENTARY NOTES Contracting Officer's Representative Dr. Paul Fedele DRDAR-CLB-PO 301-671-2262		
19. KEY WORDS (Continue on reverse side if necessary and identify by block number) Wetting; Spread rate; Flow of non-Newtonian fluid; Drop evolution; Spreading of drops; non-Newtonian drops.		
20. ABSTRACT (Continue on reverse side if necessary and identify by block number) Polymers, which are added to liquids to control the liquid's dissemination properties, also alter the rheological properties of the liquid. The polymer solutions exhibit such non-Newtonian properties as shear thinning and normal stress, which are not included in the usual Newtonian fluid model. This report evaluates theoretically how these non-Newtonian properties affect the spreading of liquid drops on ideal surfaces. Using the lubrication approximation, the		

Conte

## 20. ABSTRACT (continued)

spread rates and size doubling times are numerically calculated. Results show that shear thinning and normal stresses are considerably less important than the zero-shear-rate viscosity, and affect the spreading only during the initial spreading period, during which the drop is less than twice its original size. The viscosity's shear dependence and the normal stresses cause the size doubling time to change by less than 10% of the size doubling time of a similar drop of Newtonian liquid. The approach to the final state, and the final state itself are most strongly influenced by the zero-shear viscosity, the initial contact angle and the dependence of the contact line speed on the contact angle. Spreading on a tilted surface is also examined and it is found to be accountable by the addition of a translational motion to the spreading motion on the previously considered horizontal surface.





**Blank**

## CONTENTS

	Page
1. INTRODUCTION. . . . .	7
2. MECHANICS OF SPREADING. . . . .	8
2.1 Contact-Angle "Pull". . . . .	8
2.2 Capillary Spread. . . . .	8
3. RHEOLOGY. . . . .	8
3.1 Stress Relaxation . . . . .	10
3.2 Normal Stresses . . . . .	10
3.3 Shear Thinning. . . . .	10
4. THE MODEL OF THE DROP . . . . .	10
5. PARAMETERS. . . . .	11
6. RESULTS . . . . .	13
6.1 Two Dimensional Newtonian Drops . . . . .	14
6.2 Axisymmetric Newtonian Drops. . . . .	20
6.3 Two Dimensional Viscoelastic Drops. . . . .	31
6.4 Axisymmetric Viscoelastic Drops . . . . .	31
6.5 Effects of Gravity on Newtonian Drops on Horizontal Planes. . . . .	37
6.6 Effects of Gravity on Newtonian Drops on Tilted Surfaces. . . . .	37
7. CONCLUSIONS . . . . .	43
APPENDIX. . . . .	47
DISTRIBUTION LIST . . . . .	71

Blank

## FUNDAMENTALS OF NON-NEWTONIAN LIQUID FLOW ON SURFACES

### 1. INTRODUCTION

Chemical agents are delivered to targets in a number of different ways. A common feature of the delivery protocols is that the agents originally constitute a large bulk of liquid, which is then somehow fragmented or atomized, resulting in a cloud or array of small liquid drops. In order to ensure that the drop sizes are large enough (1mm to 3mm) that evaporation is not dominant, relatively large amounts of polymer are added to the bulk liquid. The presence of the polymer directly affects the process of break-up into droplets, and thus control the size distribution of the drops.

As the drops are propagated through the environment or fall under the influence of gravity, they respond to change in the ambient temperature, pick up contaminants from the atmosphere and lose mass due to evaporation. Eventually they strike targets, generally solid surfaces, adhere to these surfaces, begin to spread.

In order to devise a procedure for the protection from and clean-up of these agents, one must understand what controls the spreading process and in particular the parameters that govern the rate of spreading. In effect, the clean-up process is a spreading process in reverse; the removal of a drop depends on similar parameters to those which control spreading.

In the present work we investigate the spreading of non-Newtonian drops on smooth surfaces. The spreading rate thus depends on the surface tension of the liquid-air interface, the contact-angle characteristics of the solid-liquid-air system and the material properties of the liquid. In particular we assess the effects on spreading of viscoelastic properties of the liquid and examine the influence of gravity.

The general features of the spreading-drop model are described in the body of this report, together with a presentation and discussion of the results of the calculations. The details of the calculations are given in the Appendix.

## 2. MECHANICS OF SPREADING

Drops that strike a smooth solid spread through two joint mechanisms, contact-angle "pull" and capillary forces. Both contact-angle "pull" and capillary spread are included in the present model.

### 2.1 Contact-Angle "Pull"

Figure 1 shows typical measurements of contact angle  $\theta$  versus contact line speed  $u_{CL}$  for liquid-gas systems. When liquid displaces gas  $u_{CL} > 0$  and angle increases with speed. The advancing angle  $\theta_A$  is the limiting angle for  $u_{CL} \rightarrow 0$ . Thus, a drop placed on a solid with initial angle  $\theta_0 > \theta_A$  corresponds to a contact line with positive (outward) speed and the drop is pulled outward at the contact line.

### 2.2 Capillary Spread

If the drop hits the solid and  $\theta_0 = \theta_A$ , the drop will spread as long as the drop does not have the shape of a stable meniscus. Surface tension modifies the shape, steepens the contact angle and spreading results.

## 3. RHEOLOGY

There are three general features common to the motion of non-Newtonian fluids: stress relaxation, normal stresses and shear thinning. In the present formulation we employ a one parameter family of generalized Maxwell fluids, each having a single relaxation time  $\tau$ . These models include all three non-Newtonian effects while limiting cases suppress either stress relaxation or shear thinning.

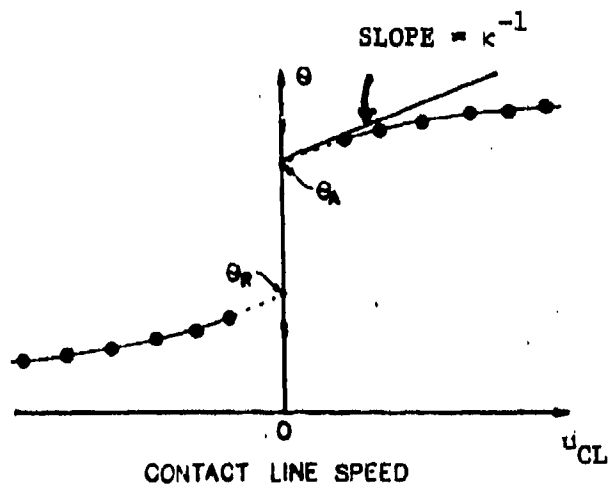


Figure 1: Illustration of how contact line speed varies with contact angle

### 3.1 Stress Relaxation

Stress relaxation is the time-dependent adjustment to rapid changes in stress, the time scale (scales) dependent on the relaxation time (times) of the material.

### 3.2 Normal Stresses

Normal stresses are stresses that develop in, say, pure shear flows in directions orthogonal to the applied force and are generated by the nonlinear behavior of the material.

### 3.3 Shear Thinning

The nonlinear behavior further allows the decrease of the apparent shear viscosity  $\mu$  with shear rate  $\dot{\gamma}$ .

## 4. THE MODEL OF THE DROP

The drops of immediate interest are ones that have small initial angle  $\theta_0$  and spread indefinitely (to final angle zero). We thus use an approximate theory valid for drops whose shapes always have small slopes, the so-called lubrication approximation. The method involves a systematic asymptotic analysis which shows that inertial effects in the liquid are negligible. More importantly, it shows that if shear thinning behavior is present, then it is more important than stress relaxation or normal stresses. Thus, in this case the main rheological data required is the zero shear rate viscosity  $\mu_0$  and the changes of  $\mu$  with shear rate. On the other hand, if the model uses a constitutive relation for which shear thinning (and hence normal stresses) are absent, the stress relaxation dominates.

The present model thus incorporates viscous, rheological and surface tension effects in the spreading process. The result of lubrication

analysis is a simplified set of nonlinear partial differential equations (plus initial and boundary conditions) that require numerical methods for solution. This system contains six non-dimensional parameters.

## 5. PARAMETERS

The dimensional quantities that enter the model are as follows:

$\rho$	density of the liquid.
$\mu_0$	zero-shear-rate viscosity of the liquid.
$\sigma$	surface tension of the liquid-gas interface.
$\kappa$	reciprocal of the slope at $u_{CL} = 0$ for the characteristic $\theta$ versus $u_{CL}$ as shown in Figure 1. $\kappa$ has units of velocity.
$\theta_A$	advancing contact angle of the drop.
$\tau$	relaxation time of the liquid.
$g$	magnitude of the gravitational acceleration.
$V^*$	volume of the drop.
$a_0$	initial radius of the drop.
$\theta_0$	initial contact angle of the drop.

The above ten dimensional quantities form into six non-dimensional groups that characterize the spreading of drops. These are as follows:

$C = \frac{\mu_0 \kappa}{\sigma \theta_0^2}$	capillary number
$\lambda = \frac{\tau \sigma \theta_0^3}{a_0 \mu_0}$	relaxation parameter #1
$\epsilon = \frac{\tau \sigma \theta_0^2}{a_0 \mu_0}$	relaxation parameter #2

$$B = \frac{\rho g a_0^2}{\sigma}$$

Bond number

$$\theta_F = \theta_A / \theta_0$$

final contact angle

$$V = \begin{cases} \frac{V^*}{a_0^3 \theta_0} \\ \frac{V^*}{a_0^2 \theta_0} \end{cases}$$

volume of the (axisymmetric) drop

volume per unit depth of the (two-dimensional) drop.

The capillary number expresses the relative importance of contact-angle "pull", measured by speed  $\kappa \theta_0$ , to capillary spread, measured by  $\sigma \theta_0^3 / \mu_0$ . The relaxation parameter #1 measures the relaxation time  $\tau$  versus capillary effects. The relaxation parameter #2 measures the relaxation time  $\tau$  for shear thinning versus capillary effects. Notice that  $\lambda / \epsilon = \theta_0$  and since  $\theta_0$  is very small, stress relaxation effects are small compared to those due to shear thinning except when the latter are absent. The Bond number measures the effects of gravity (compared to surface tension) when the plate is horizontal. We allow the possibility that the drop ceases spreading at final angle  $\theta_F$ . If  $\theta_F = 0$ , the drop spreads indefinitely.

In order to see the ranges of values taken by the various parameters, we write down "typical" values for the dimensional quantities. We use  $a_0 = 0.25$  cm,  $\theta_0 = 0.1$  rad =  $5.7^\circ$ ,  $V^* = 1.5 \times 10^{-4}$  cm<sup>3</sup>,  $\sigma = 30$  dynes/cm,  $\mu_0 = 5$  poise and  $\rho = 1$  gm/cm<sup>3</sup>. We have no information on the contact angle constant  $\kappa$ ; we take  $\kappa = 0.1$  cm/sec. The relaxation time  $\tau$  can be obtained from data on apparent viscosity versus shear rate and equation (2.44) of the Appendix if we rewrite it in dimensional form. The apparent viscosity  $\mu$  of our model takes the form

$$\mu = \frac{\mu_0}{1 + \tau \dot{\gamma}^2} \quad (1)$$

where  $\mu_0$  is the zero-shear-rate viscosity and  $\dot{\gamma}$  is the shear rate. From the CSL data given to us, we estimate for Diethylmalonate thickened with 2.1% Polymethylmethacrylate that  $\tau = 1.0$  sec; for Diethylmalonate thickened with 5.2% Copolymer,  $\tau = 0.013$  sec; for Diethylmalonate thickened with 9.5% Elvacite 2041,  $\tau = 0.0063$  sec; for Methyl Salicylate thickened with 4.5% Copolymer,  $\tau = 0.010$  sec. Thus, a practical upper limit for  $\tau$  is about 1 sec. With this estimate we find that "typical" values for the parameters are as follows:

$$\begin{aligned} C &\approx 1.6 \\ \lambda &\approx 2.5 \times 10^{-2} \\ \epsilon &\approx 2.5 \times 10^{-1} \\ B &\approx 2.1 \\ v &\approx 1.0 \end{aligned} \quad (2)$$

Clearly, the estimates (2) are crude and each parameter has a range of possible values. We shall use  $\epsilon = 5.0$ , a very large value for the calculations in order to exaggerate the effects of viscoelasticity.

## 6. RESULTS

We use the spreading of a Newtonian liquid drop as the standard against which to compare results for non-Newtonian cases. We thus first present results for this case. Since spreading rates depend explicitly on time we shall define a non-dimensional time  $t$  in terms of the dimensional time (sec)  $t^*$  as follows:

$$t = \frac{\sigma_0^3 t^*}{a_0 \mu_0} \quad (3)$$

In terms of the typical values of parameters given in Section 5,  $t = 1$  corresponds to physical time  $t^*$  about 2.5 seconds.

### 6.1 Two-Dimensional Newtonian Drops

The discussion here relates to a Newtonian constitutive model in which the viscosity  $\mu_0$  is constant, but  $\mu_0$  should be regarded for purposes of comparison as the zero-shear-rate viscosity of the real liquid.

Figures 2a and 2b show the shape of the drop at various instants of time  $t$  for the case  $V = 0.75$ ,  $C = 1$ ,  $\lambda = \epsilon = B = 0$ . In Figure 2a the final angle  $\theta_F = 0.5$  and so the drop shape approaches a static equilibrium as  $t \rightarrow \infty$ . In Figure 2b, the final angle  $\theta_F = 0$  and so the drop spreads indefinitely. These Figures refer to the early stages of the drop's spread. By contrast we illustrate in Figures 3a and 3b the shape of the drop when substantial spread has occurred. In these two Figures we have taken  $\theta_F = 0$ ,  $C = 1$ ,  $\lambda = \epsilon = B = 0$ , and we show the shape of the drop when  $t = 0$  and when  $t = t^{(2)}$ , where  $t^{(2)}$  is the time for the drop to spread to a size twice its initial radius. We shall call  $a(t)$  the radius of the drop even though in two dimensions it is really the half-width of the drop. Note that  $a(0)/a_0 = 1$  by definition. In Figure 3a we have taken  $V = 0.75$ , while  $V = 1.0$  in Figure 3b.

Graphs such as the above give qualitative information but quantitative predictions must be extracted.

First, we examine cases,  $\theta_F = 0$ , for which the drop spreads indefinitely. We set  $\lambda = \epsilon = B = 0$  and examine  $t^{(2)}$  as functions of both  $C$  and  $V$ . Figure 4 shows  $t^{(2)}$  versus  $V$  for several values of  $C$ . The spreading rate depends strongly on the volume of the drop (for fixed initial contact angle  $\theta_0$ ), large drops spread faster than smaller drops. Also, for a fixed volume of liquid the time it takes to double the initial radius

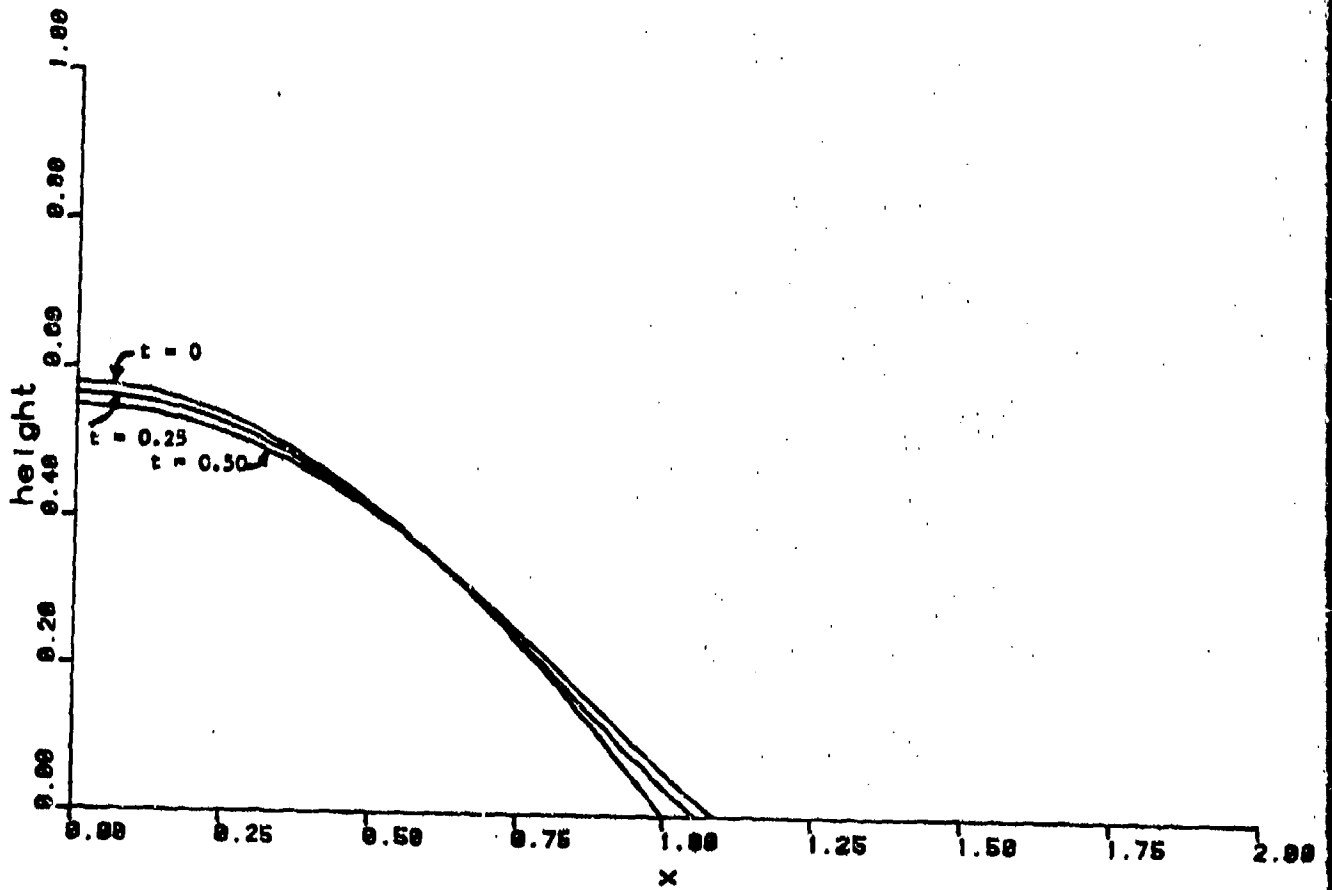


Figure 2a: Two-dimensional drop, shapes in early stages of spread for  
 $v = 0.75, C = 1, \lambda = \epsilon = B = 0, \theta_F = 0.5$

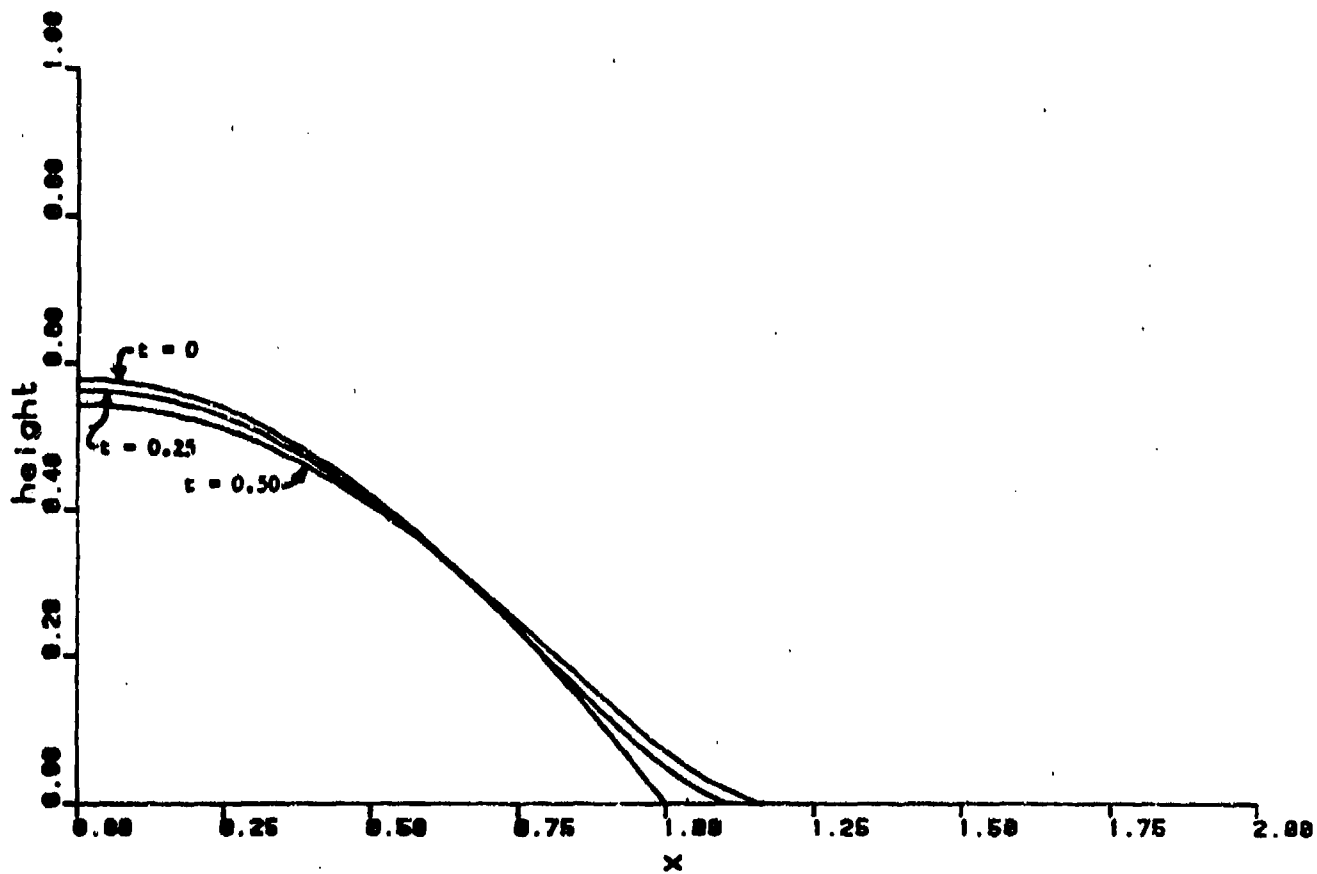


Figure 2b: Two-dimensional drop, shapes in early stages of spread for  
 $V = 0.75, C = 1, \epsilon = \lambda = B = 0, \theta_F = 0.0$

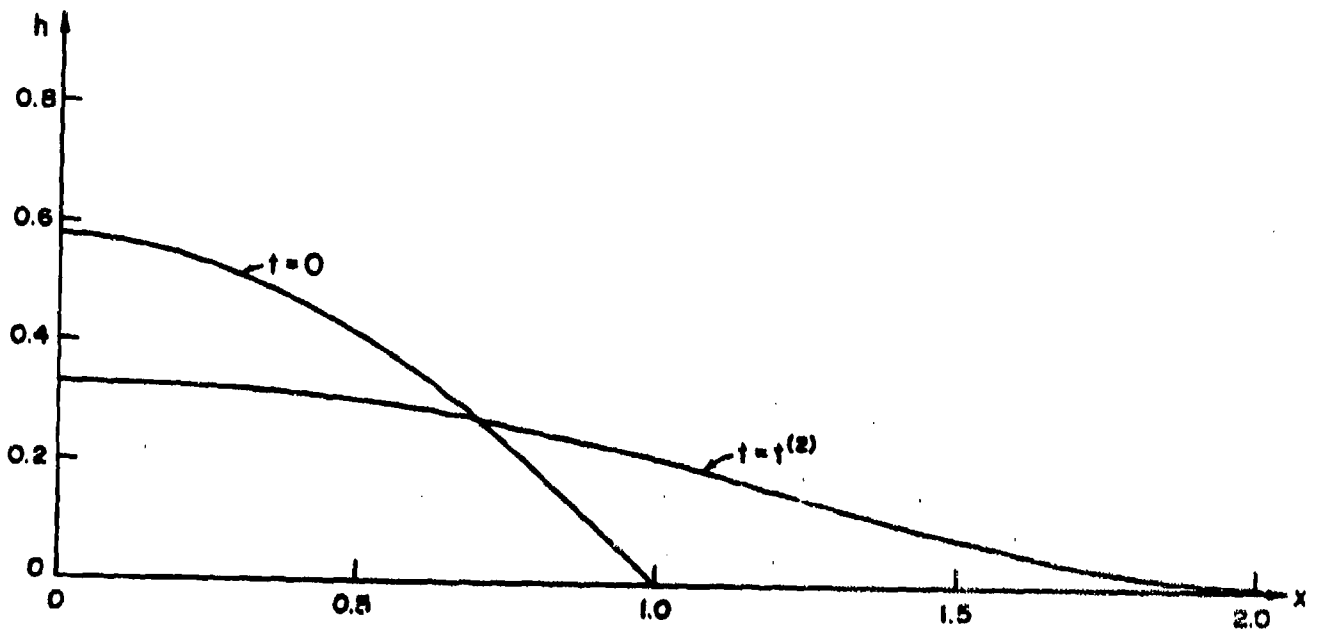


Figure 3a: Two-dimensional drop, shapes at  $t = 0$  and  $t = t^{(2)}$  for  
 $V = 3.75, C = 1, \epsilon = \lambda = B = 0$

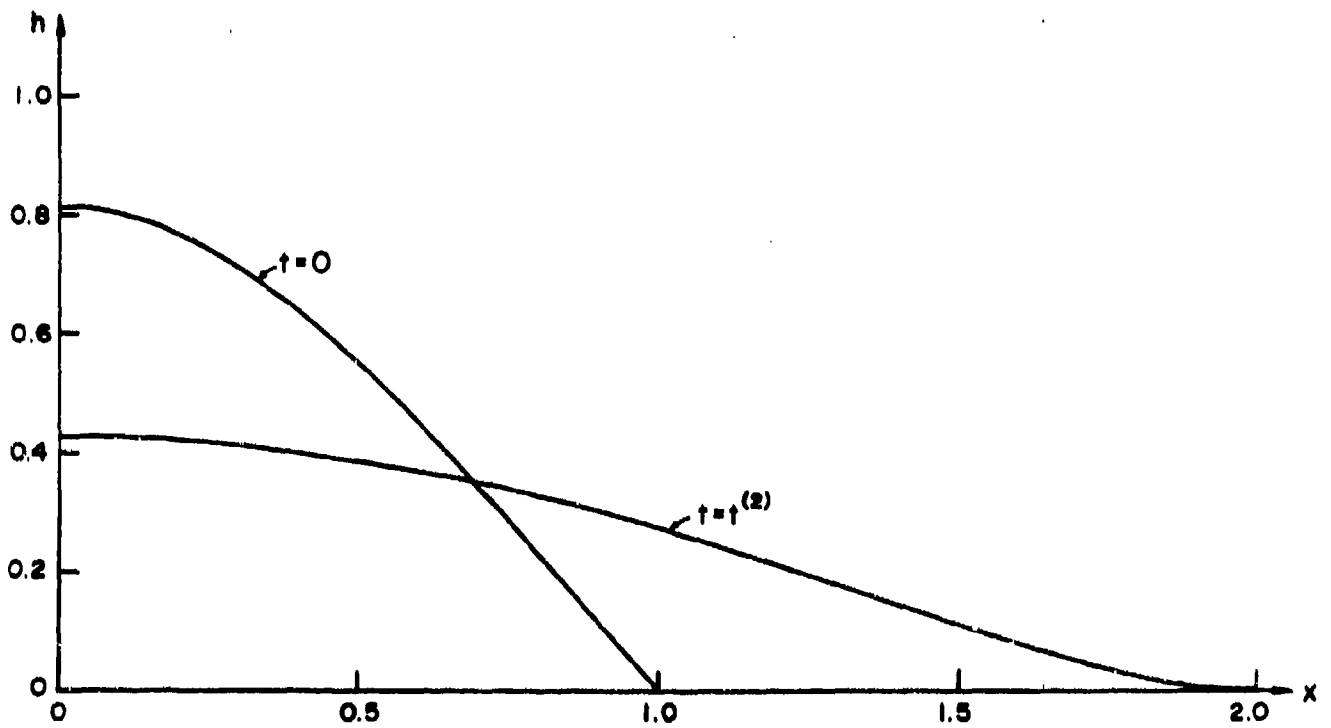


Figure 3b: Two-dimensional drop, shape at  $t = 0$  and  $t = t^{(2)}$  for  
 $V = 1, C = 1, \epsilon = \lambda = B = 0$

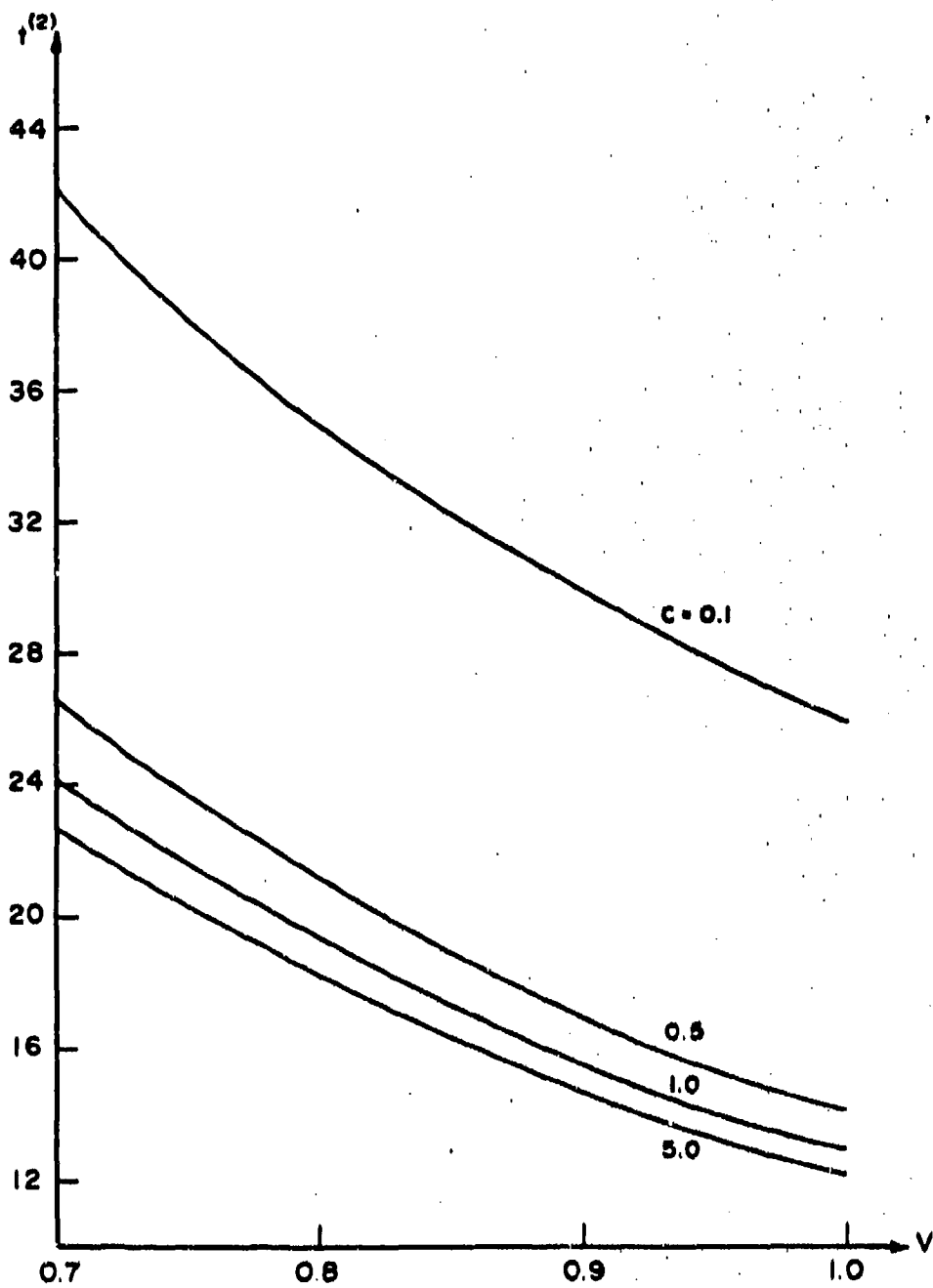


Figure 4: Two-dimensional drop, doubling time as a function of  $V$  for various  $C$ , with  $\epsilon = \lambda = B = 0$

of the drop is larger the smaller the value of  $C$ .  $C$  decreases with surface tension  $\sigma$  and increases with zero-shear-rate viscosity.

Figure 5 shows the doubling time  $t^{(2)}$  as a function of the capillary number  $C$  in the case  $V = 1$ . Figure 6 gives the radius  $a(t)$  versus  $t$  for various values of  $V$ , here for  $C = 1$ . Figure 7 shows the radius  $a(t)$  versus  $t$  for various values of  $C$ , here for  $V = 1$ . Thus, Figures 4 and 5 summarize the data of Figures 6 and 7.

In Figure 8 we extend, on a different scale, the variation of  $a(t)$  with  $t$  in the case  $V = 1$ ,  $C = 1$ .

We now examine the case for  $\theta_F \neq 0$ . Although the case  $\theta_F = 0$  is of most interest for CSL, we used cases for  $\theta_F \neq 0$  as tests of the numerics and we present some of the results here.

We confine our attention to  $\lambda = \epsilon = B = 0$  and take  $\theta_F = 0.5$ . Figure 9 shows the radius of the drop as a function of time for various  $V$  with  $C = 1$ . The vertical lines are the asymptotes valid for  $t \rightarrow \infty$ . There seems to be little qualitative difference between cases  $\theta_F = 0$  and  $\theta_F \neq 0$  until one approaches times large enough that the finite equilibrium is closely approached.

## 6.2 Axisymmetric Newtonian Drops

Figures 10-14 give for the axisymmetric drop the information equivalent to Figures 4-8 of the two-dimensional drop. The same trends persist here as in that case. Spreading is more rapid for large drops that have large capillary numbers. However, we do see that axisymmetric drops spread more slowly than their two-dimensional counterparts. For example if  $C = V = 1$ ,  $t^{(2)} = 13.0$  for the two-dimensional drop while  $t^{(2)} = 27.2$  for the axisymmetric drop.

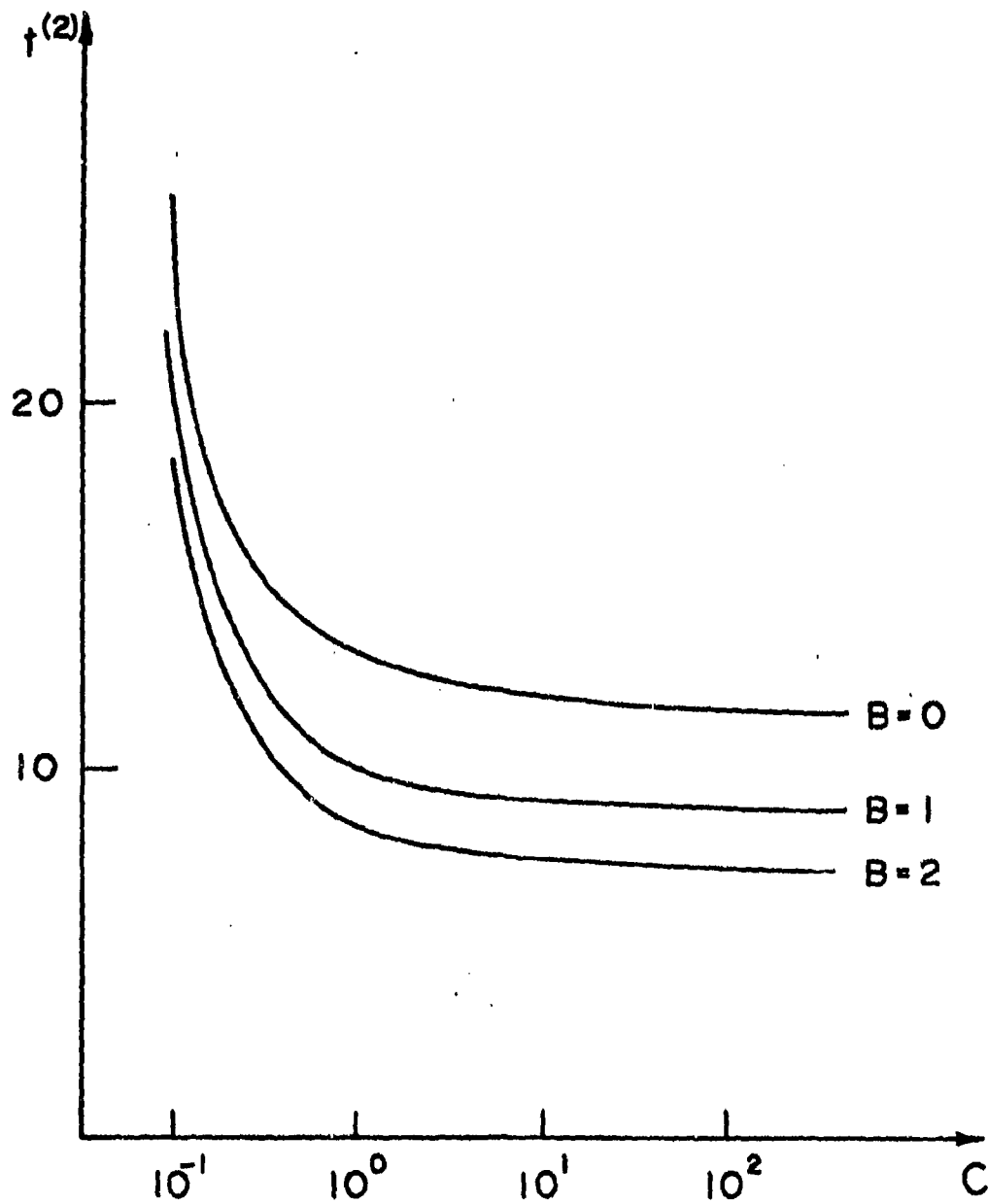


Figure 5: Two-dimensional drop, variation of doubling time with  $C$   
for various  $B$ ,  $V = 1$ ,  $\epsilon = \lambda = 0$

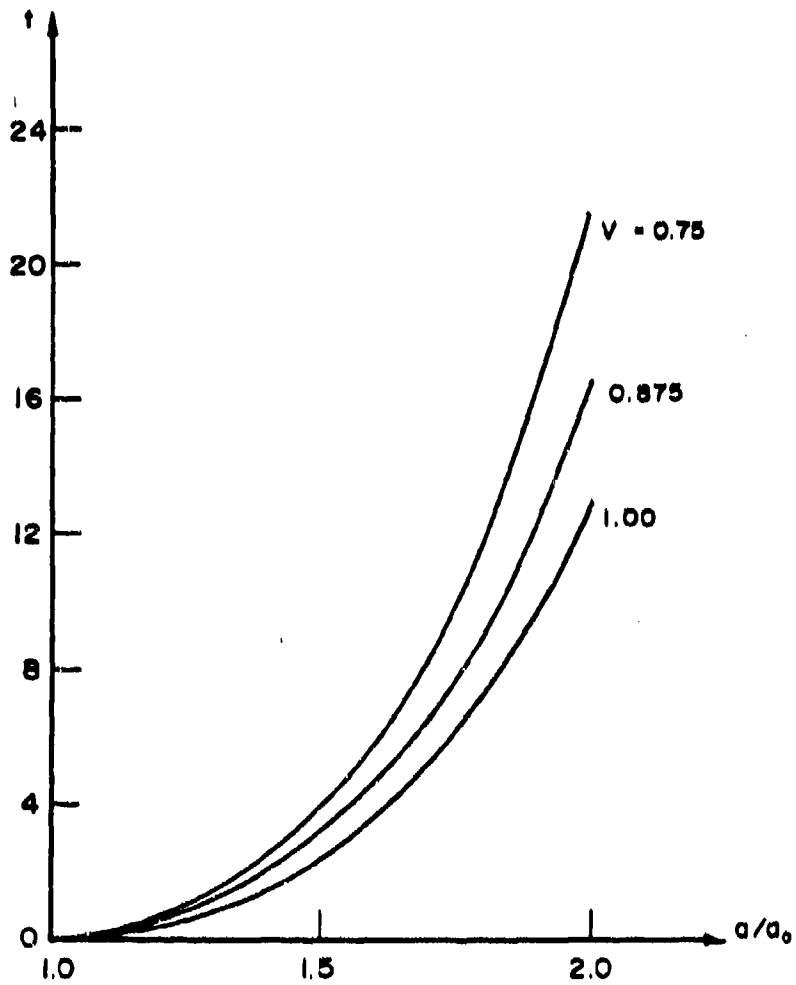


Figure 6: Two-dimensional drop, variation of radius with  $t$  for various  $V$ , with  $C = 1$ ,  $\theta_F = 0$ ,  $\epsilon = \lambda = B = 0$

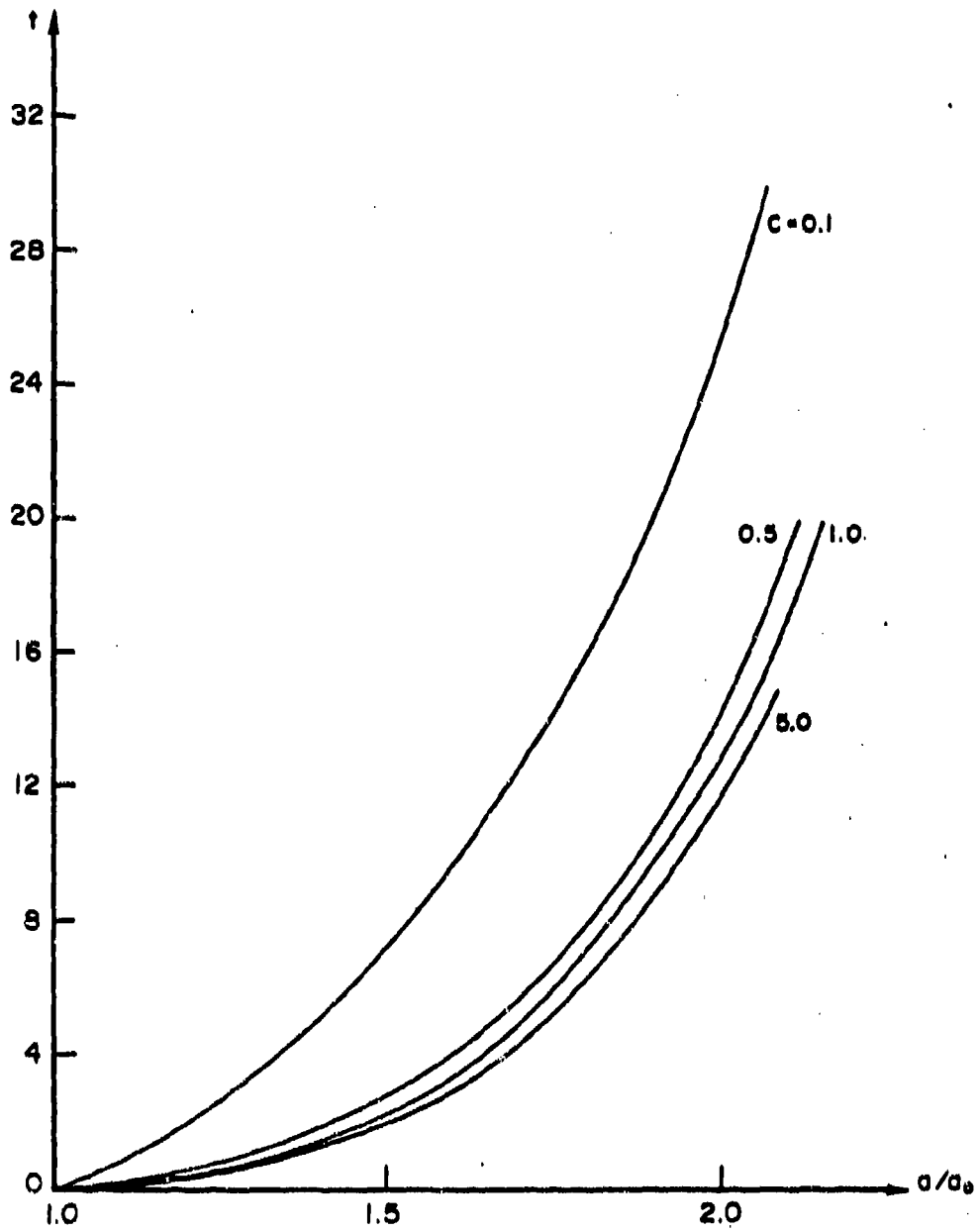


Figure 7: Two-dimensional drop, variation of radius with  $t$  for various  $C$ , with  $V = 1$ ,  $\theta_F = 0$ ,  $e = \lambda = B = 0$

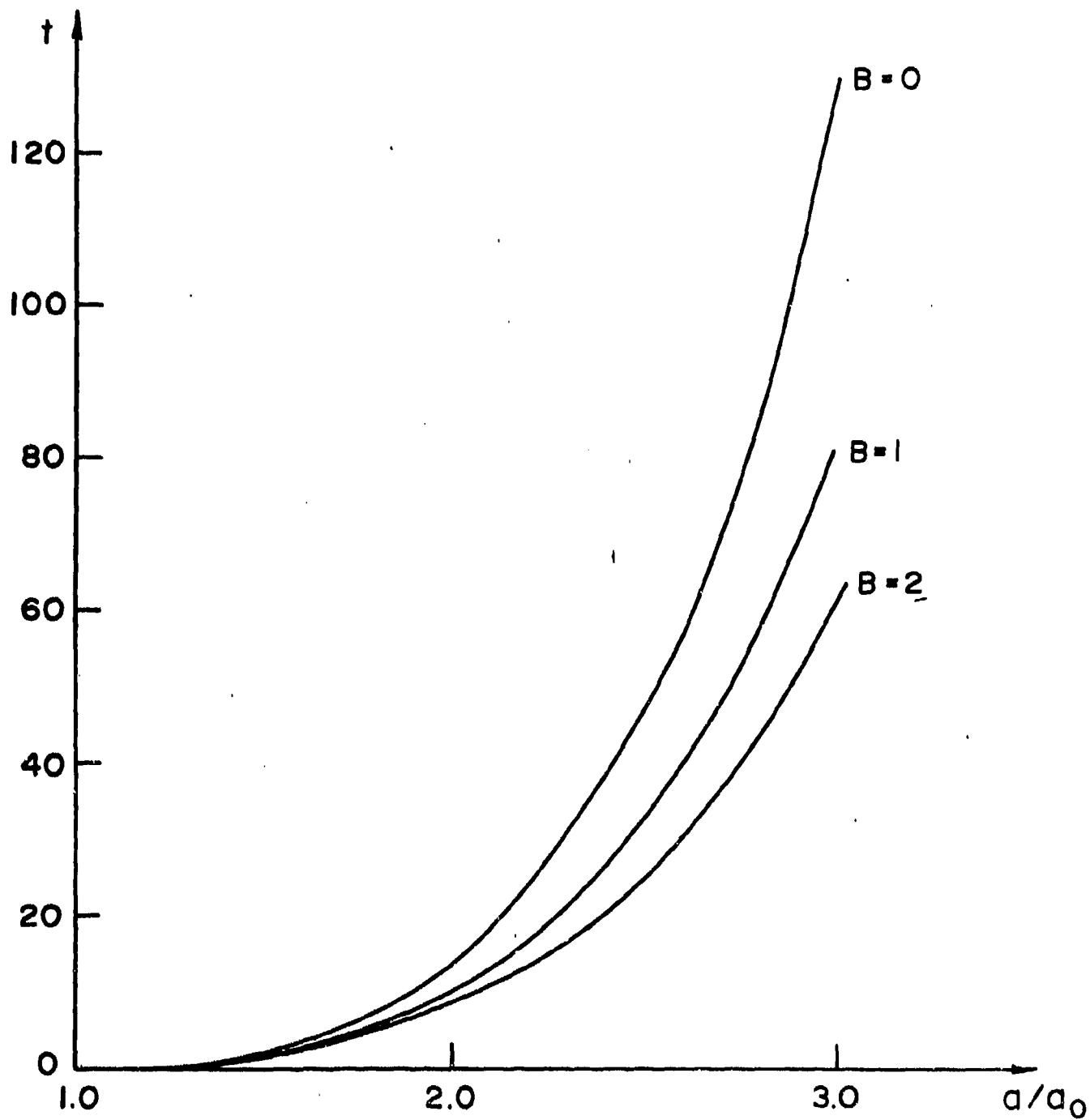


Figure 8: Two-dimensional drop, time rate of change of radius for various  $B$ , with  $C = 1$ ,  $V = 1$ ,  $\varepsilon = \lambda = 0$

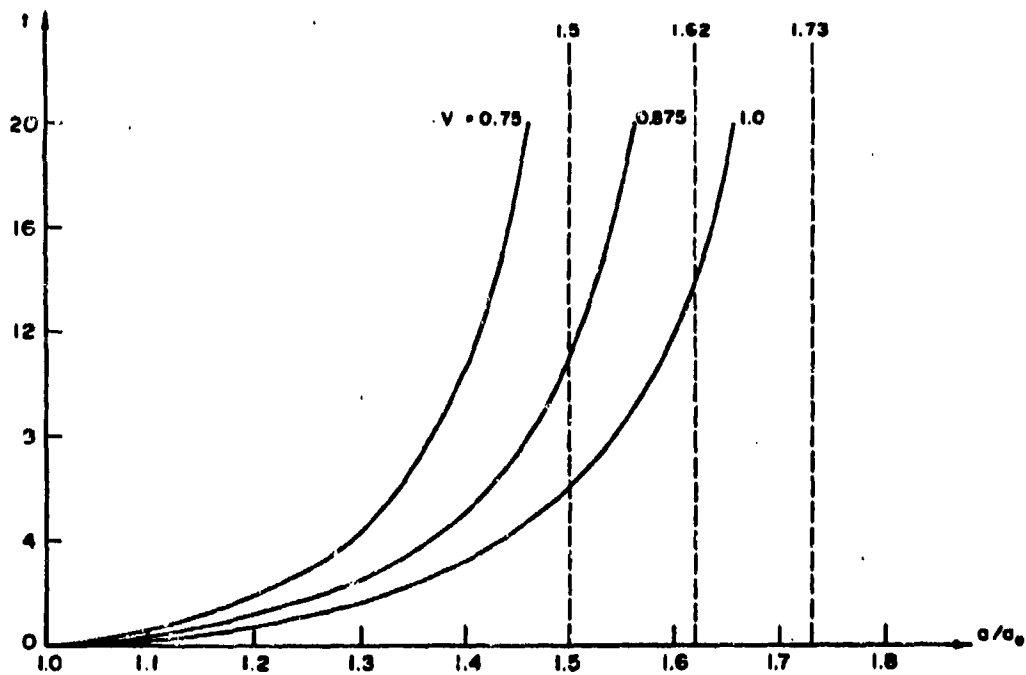


Figure 9: Two-dimensional drop, radius as a function of time for  $\theta_F = 0.5$  and various  $V$ , with  $C = 1$ ,  $\epsilon = \lambda = B = 0$

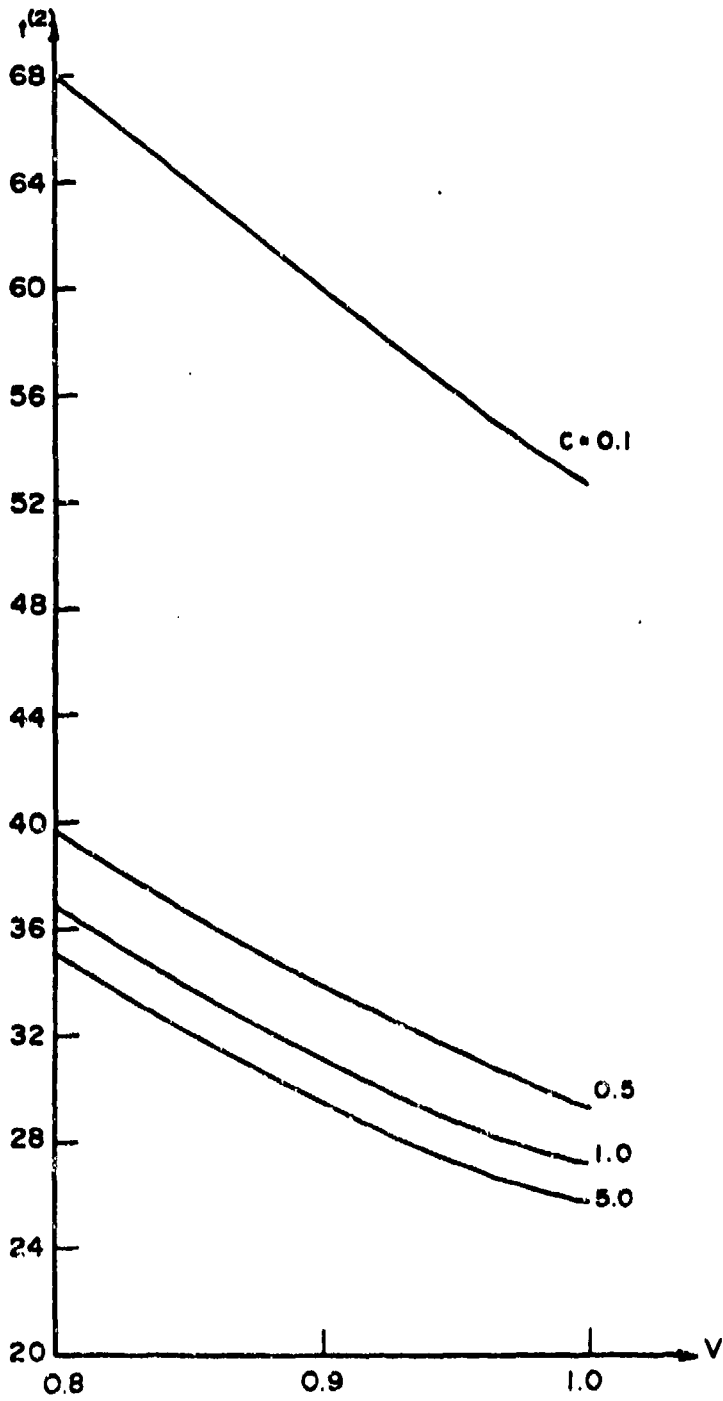


Figure 10: Axisymmetric drop, doubling time as a function of  $V$  for various  $C$ , with  $\varepsilon = \lambda = B = 0$

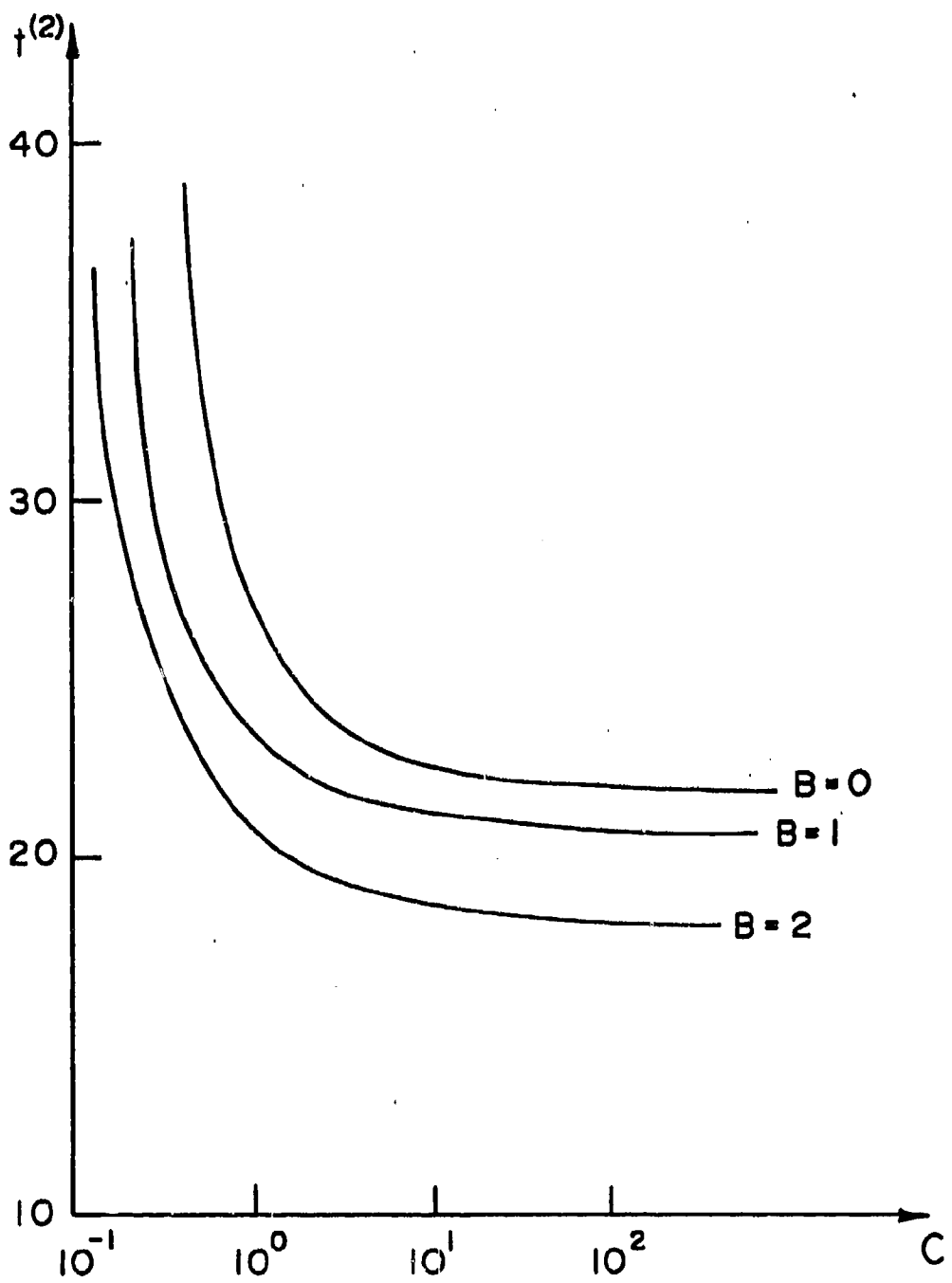


Figure 11: Axisymmetric drop, doubling time variation with  $C$  for various  $B$ , with  $V = 1$ ,  $\varepsilon = \lambda = 0$

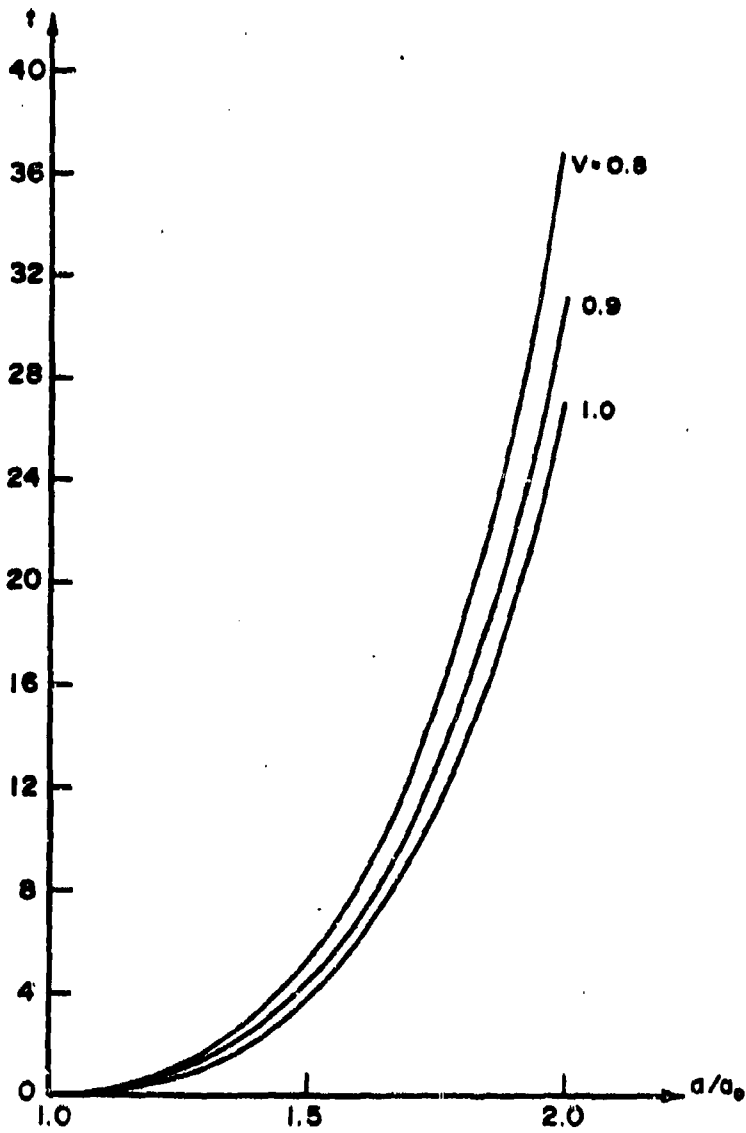


Figure 12: Axisymmetric drop, variation of radius with  $t$  for various  $V$ ,  
 with  $C = 1$ ,  $\theta_F = 0$ ,  $\varepsilon = \nu = B = 0$

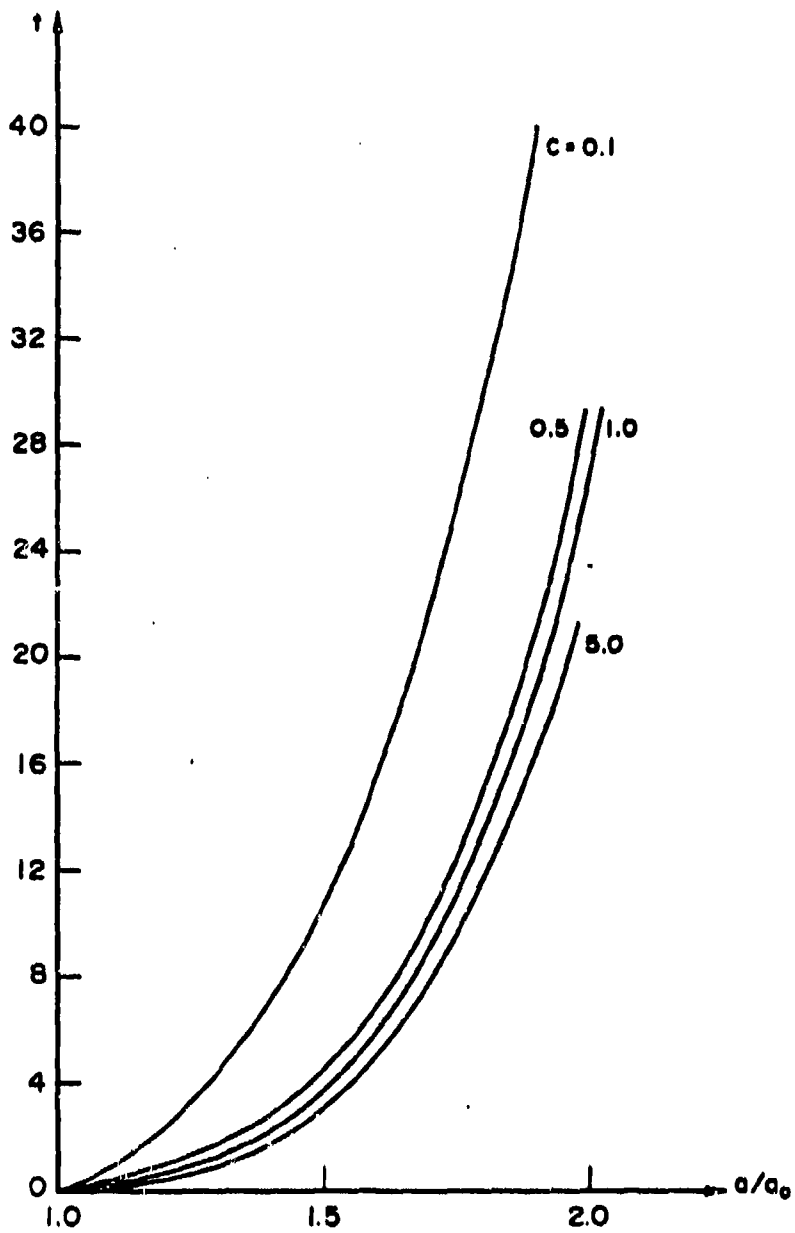


Figure 13: Axisymmetric drop, variation of radius with  $t$  for various  $C$ , with  $V = 1$ ,  $\theta_F = 0$ ,  $\epsilon = \lambda = B = 0$

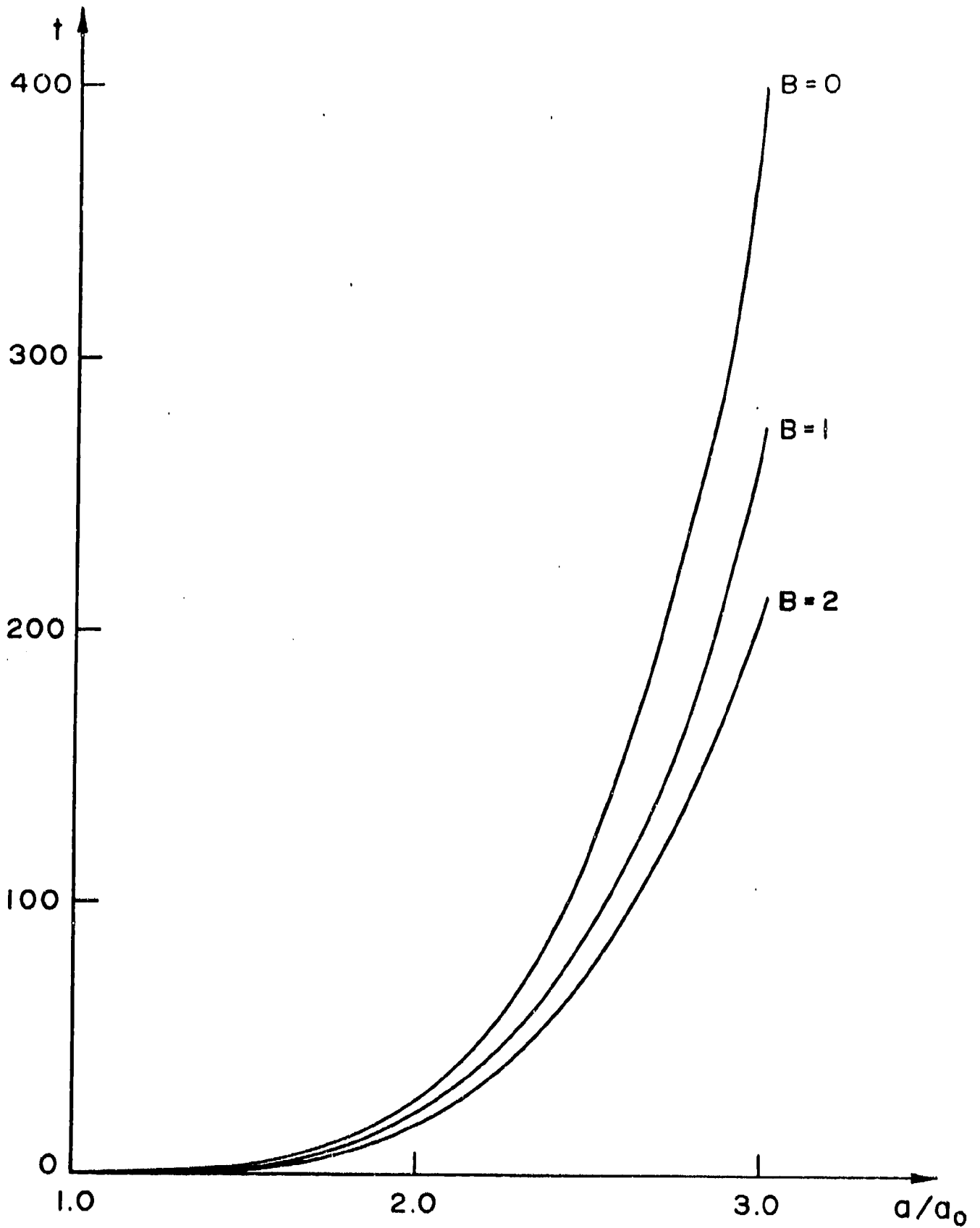


Figure 14: Axisymmetric drop, time-rate of change of radius for various  $B$ , with  $C = 1$ ,  $V = 1$ ,  $\epsilon = \lambda = 0$

### 6.3 Two-Dimensional Viscoelastic Drops

The constitutive model used here contains a single relaxation time which enters the governing equations through two parameters, the relaxation parameters  $\lambda$  and  $\epsilon$ . Recall that  $\lambda$  is formally much smaller than  $\epsilon$  by a factor  $\theta_0$ .

We now present spreading curves for non-Newtonian cases and compare these with the corresponding Newtonian cases. Figure 15 shows the radius of the drop as a function of  $t$  for three cases with  $C = V = 1$ ,  $B = 0$ ,  $\theta_F = 0.5$ . There is the Newtonian case  $\epsilon = \lambda = 0$ , a stress-relaxation case  $\epsilon = 0$ ,  $\lambda = 0.5$  and a shear thinning case  $\epsilon = 5.0$ ,  $\lambda = 0$ . Firstly, we see that for equal values for the material relaxation time  $\tau$  and for, say,  $\theta_0 = 0.1$  that  $\epsilon = 10\lambda$  and the effect of shear thinning is much larger than that of stress relaxation. Shear thinning causes the drop to spread faster than the corresponding Newtonian drop given that the two have equal zero-shear-rate viscosities. For example in the present example the viscoelastic drop reaches 150% of its initial radius when  $t = 4.0$  while the corresponding drop for  $\lambda = 0$  reaches this position at  $t = 6.4$ . If stress relaxation only is considered, the drop spreads more slowly and attains 150% of its initial radius at  $t = 6.8$ . Rather than pursue ranges of parameters here, we turn to the axisymmetric drop and confine our attention to the principal case,  $\lambda = 0$ ,  $\epsilon \neq 0$ , in which shear-thinning only is present.

### 6.4 Axisymmetric Viscoelastic Drops

Figures 16-18 give results for drops that have significant shear-thinning effects  $\epsilon = 5.0$ , vanishingly small stress relaxation  $\lambda = 0$  and final contact angle  $\theta_F = 0$  so spreading continues indefinitely. Gravity

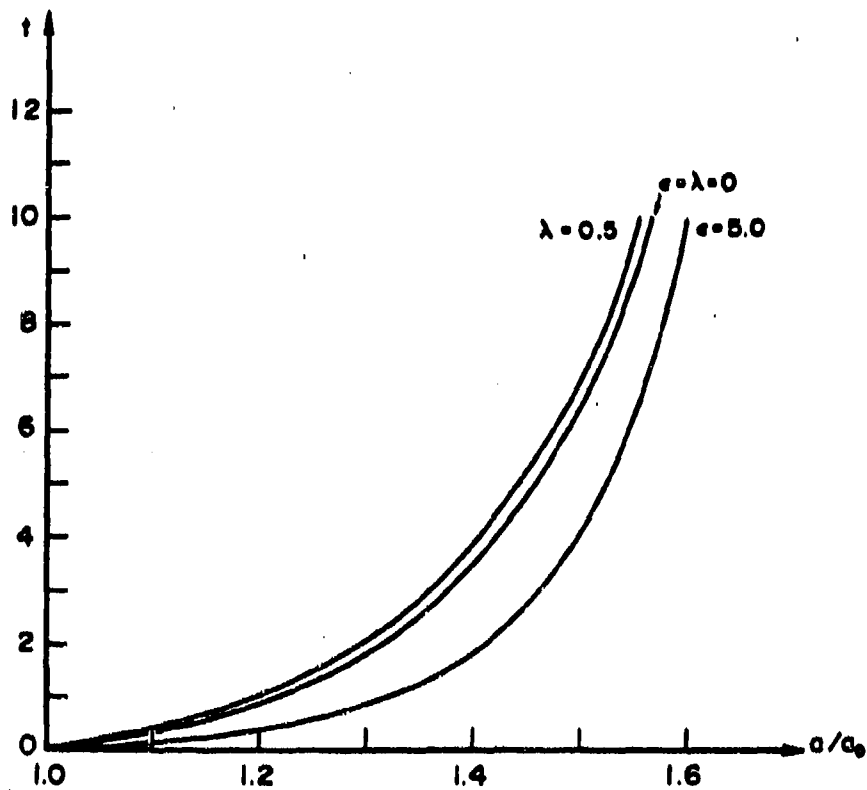


Figure 15: Two-dimensional drop, variation of radius with  $t$  for viscoelastic cases with  $\theta_F = 0$ ,  $C = 1$ ,  $V = 1$ ,  $B = 0$

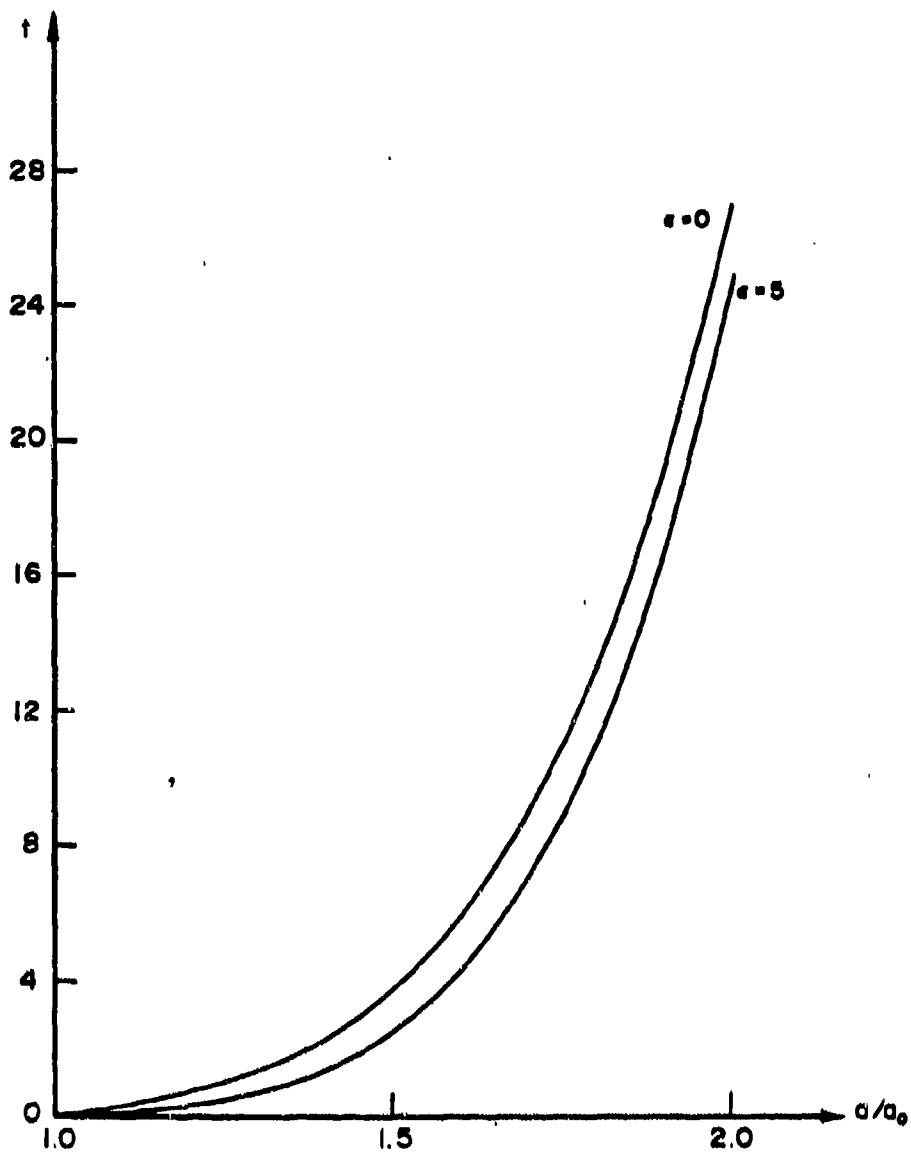


Figure 16: Axisymmetric drop, variation of radius with  $t$  for shear-thinning and non-shear-thinning cases, with  $C = V = 1$ ,  $B = 0$ ,  $\theta_F = 0$

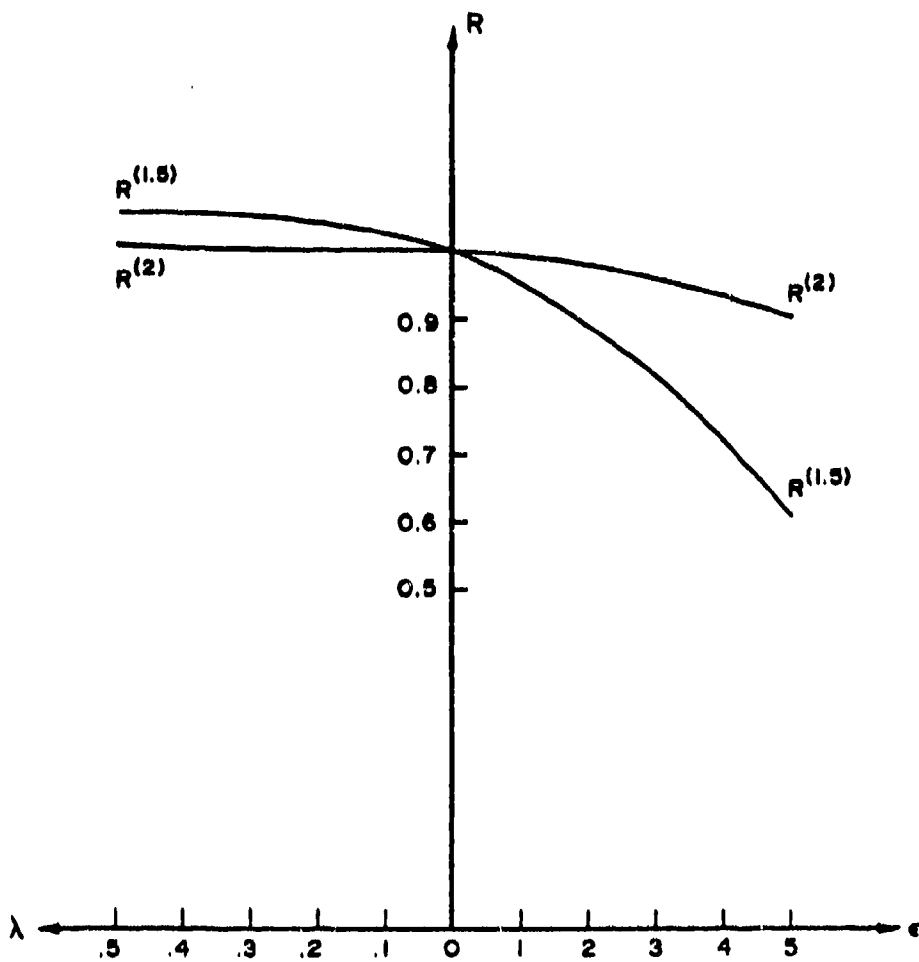


Figure 17: Axisymmetric drop, ratios of spreading times [see equation (4)]  
as functions of elasticity parameters, with  $C = 1$ ,  $V = 1$ ,  $B = 0$

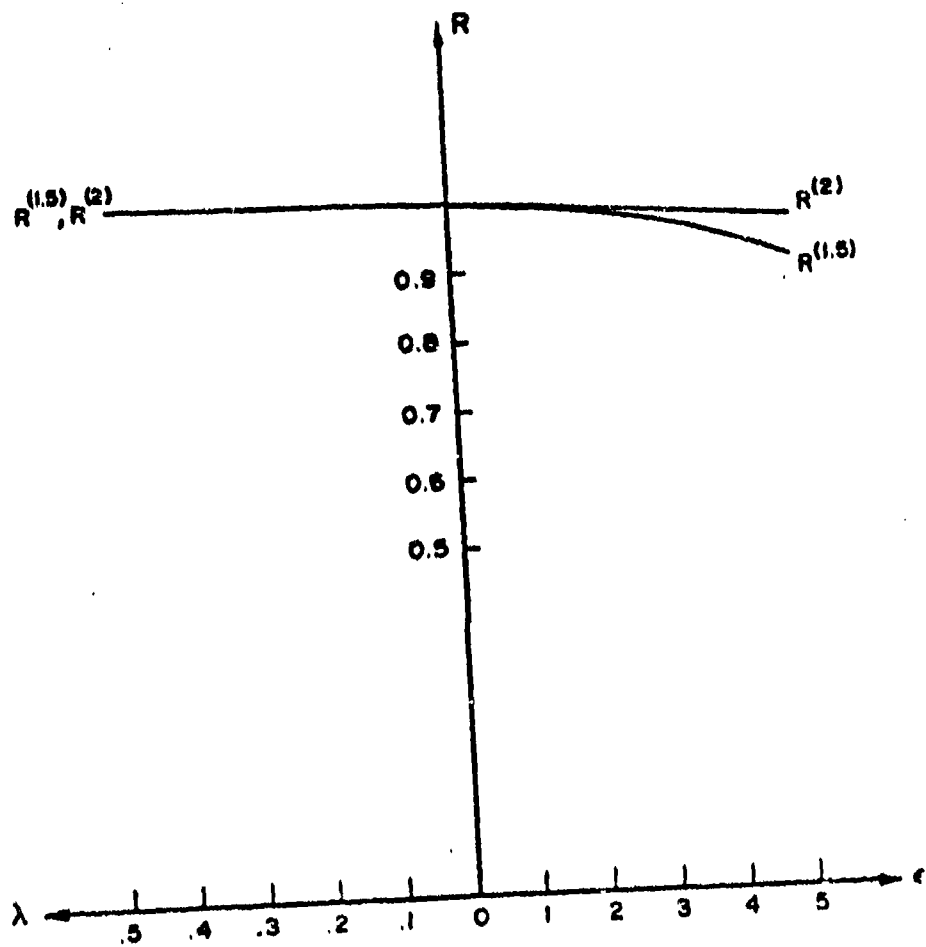


Figure 18: Axisymmetric drop, ratios of spreading times as functions of elasticity parameters, with  $C = 0.1$ ,  $B = 0$ ,  $V = 1$

is ignored,  $B = 0$ , and a range of capillary numbers  $C$  and drop volumes  $V$  is examined.

Figure 16 gives the radius  $a(t)$  of the drop as a function of time for  $B = \lambda = 0$  and  $C = V = 1$ . There are two cases shown, one for the Newtonian drop with  $\epsilon = 0$  and one for the viscoelastic drops with  $\epsilon = 5.0$ . We see that  $t^{(2)}$  decreases by about 15% due to shear thinning.

We can compare the viscoelastic cases to the Newtonian cases by defining a ratio  $R^{(2)}$ ,

$$R^{(2)} = \frac{t_{\text{VISCOELASTIC}}^{(2)}}{t_{\text{NEWTONIAN}}^{(2)}} \quad (4)$$

The quantity  $R^{(1.5)}$  is the similar ratio for a 50% increase in radius.

Figure 17 shows  $R^{(2)}$  and  $R^{(1.5)}$  for the case  $B = 0$ ,  $V = C = 1$  where the right side of the figure shows shear-thinning effects only  $\epsilon \neq 0$ ,  $\lambda = 0$  and the left side shows stress relaxation effects only,  $\epsilon = 0$ ,  $\lambda \neq 0$ . On one hand we again see that shear thinning has a larger effect than does stress relaxation. On the other hand there is a "catch-up" phenomenon present. The largest effect on spreading of viscoelasticity occurs at early times  $t$ . However, not only does viscoelasticity have weaker effects later but the differences in spread rates become smaller as time passes. Notice that  $R^{(2)}$  is nearer to unity than is  $R^{(1.5)}$ . Thus, viscoelastic drops that have had a long time to spread have attained nearly the same radii as their Newtonian counterparts. Figure 18 shows equivalent information for the case  $B = 0$ ,  $C = 0.1$ ,  $V = 1$ . Notice that the effects of viscoelasticity are much smaller here for  $C = 0.1$  than for the earlier case for  $C = 1.0$ .

### 6.5 Effects of Gravity on Newtonian Drops on Horizontal Planes

When a drop spreads on a smooth horizontal plane, gravity modifies the shape and spreading characteristics of the drop.

Figure 19 shows a two-dimensional Newtonian case for  $C = 1$ ,  $V = 0.75$  and  $B = 10$  at various times  $t$ . A comparison of these curves with those of Figure 2b for the equivalent case with  $B = 0$  shows that gravity steepens the interface near the contact line which leads to more rapid spreading. Similar behavior can be observed in Figures 20a and 20b, which are the direct analogs of Figures 3a and 3b respectively for the case  $B = 10$ .

Figures 21 and 22, respectively, show  $a(t)$  versus  $(t)$  for various values of  $B$  for two-dimensional and axisymmetric spread. Notice for  $B = 1.0$  that  $R^{(2)} = 0.76$  for the two-dimensional drop and  $R^{(2)} = 0.84$  for the axisymmetric drop so that there are comparable accelerations of spreading in both geometries due to gravity. Effects of gravity are also indicated in Figures 8 and 14, which give long-time spreading behavior, and in Figures 5 and 11, which show how doubling-time varies with capillary number.

### 6.6 Effects of Gravity on Newtonian Drops on Tilted Surfaces

A drop sits on a plane tilted an angle  $\beta$  to the horizontal. The component  $g \cos \beta$  of gravity normal to the plate leads to a Bond number  $B \cos \beta$  whose effect was discussed in Subsection 6.5. The component  $g \sin \beta$  of gravity "slides" the drop bodily down the plate as discussed by Hocking\* for the two-dimensional case with  $C \rightarrow \infty$ .

The wetting properties for  $C < \infty$  shown in Figure 1 allow the drop to make an initial adjustment in its shape to accommodate to a steady

---

\* Quart. J. Mech. Appl. Math. 34, 37, 1981

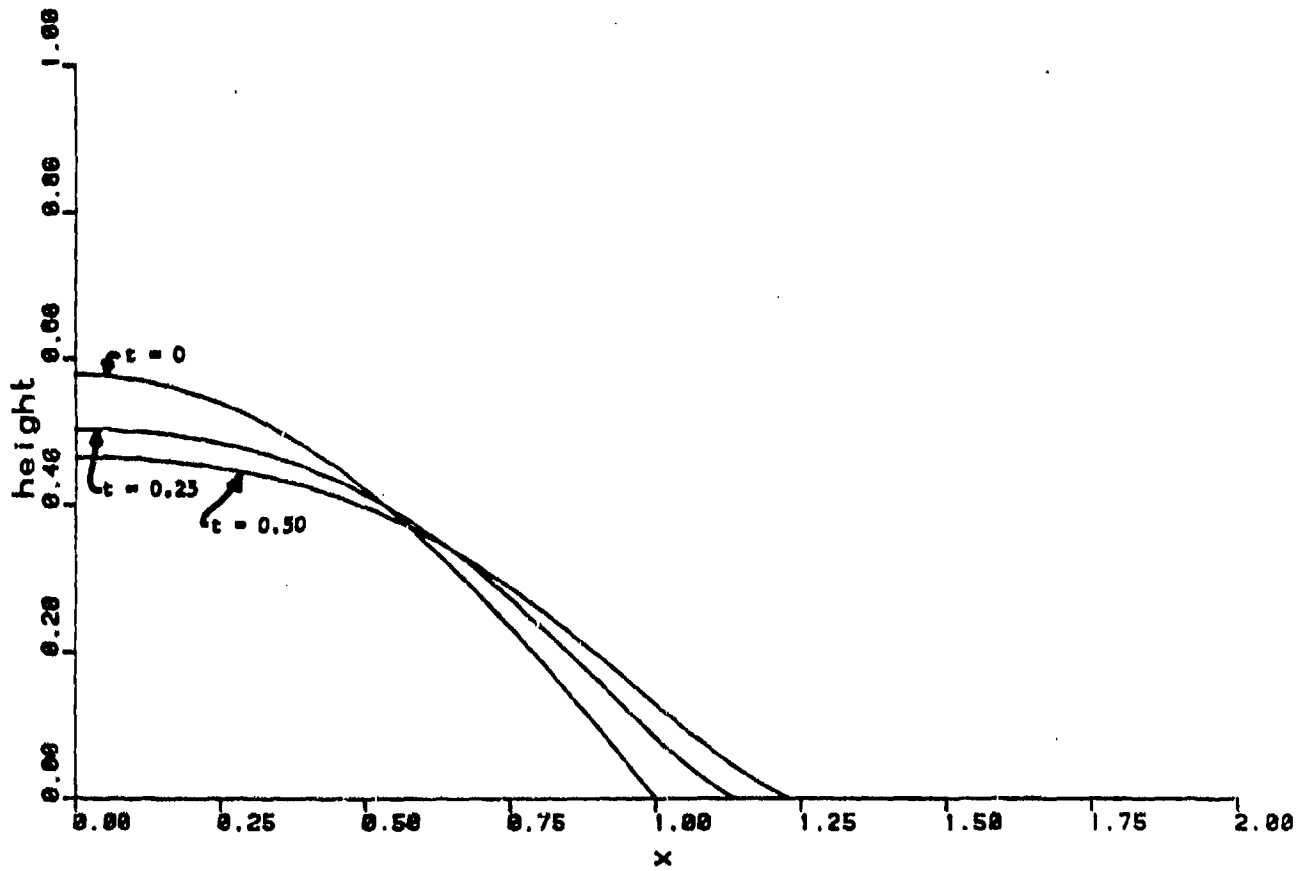


Figure 19: Two-dimensional drop, shapes in early stages of spread for  
 $V = 0.75, C = 1, B = 10, \theta_F = 0, \epsilon = \lambda = 0$

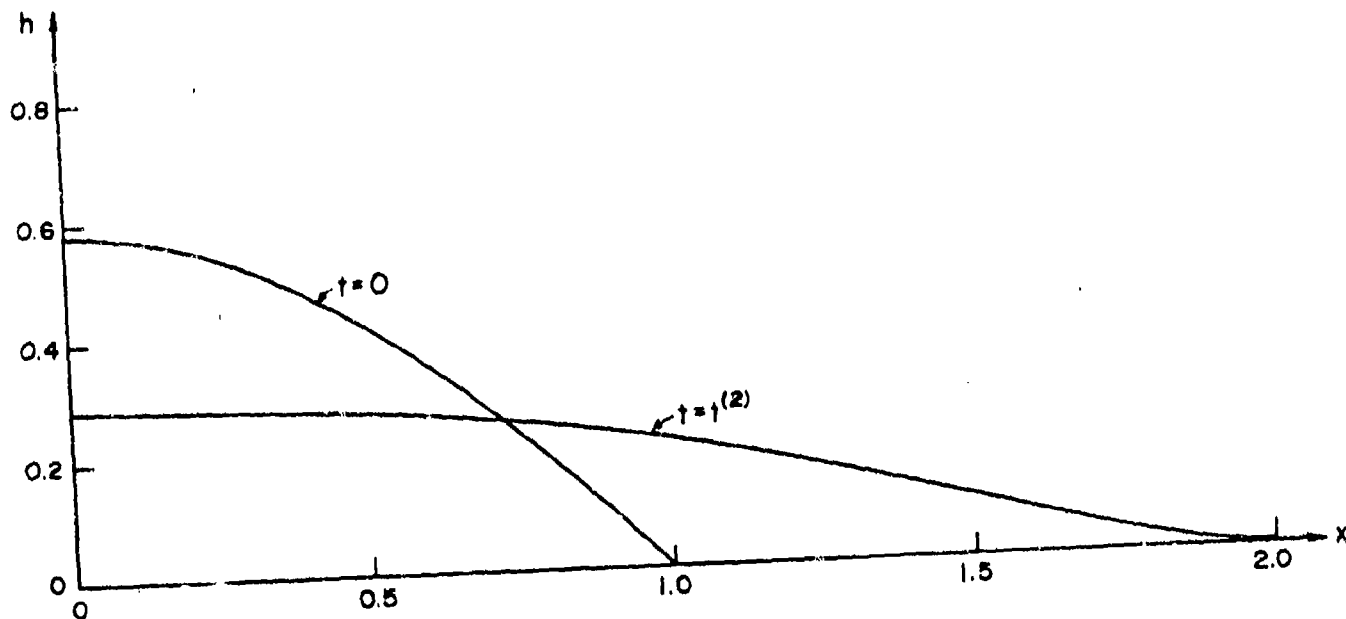


Figure 20a: Two-dimensional drop, shapes at  $t = 0$  and  $t = t^{(2)}$  for  $V = 0.75$ ,  
 $C = 1$ ,  $B = 10$ ,  $\varepsilon = \lambda = 0$

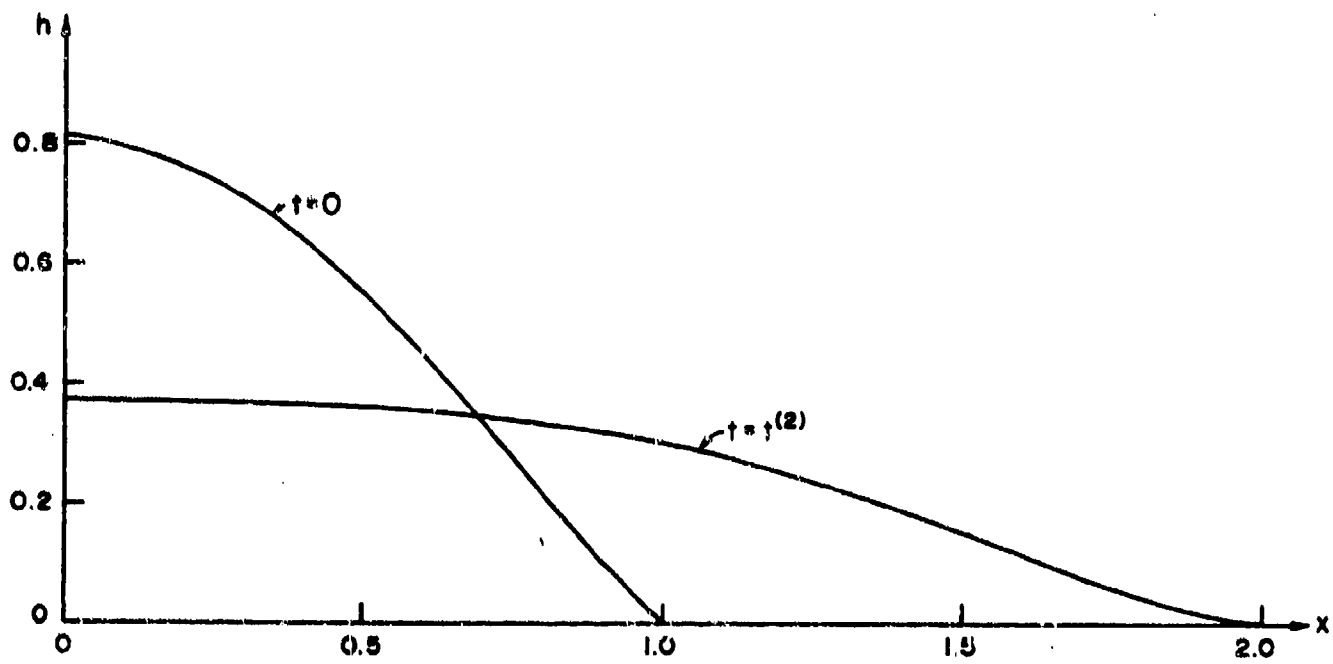


Figure 20b: Two-dimensional drop, shapes at  $t = 0$  and  $t = t^{(2)}$  for  
 $V = 1, C = 1, B = 10, \epsilon = \lambda = 0$

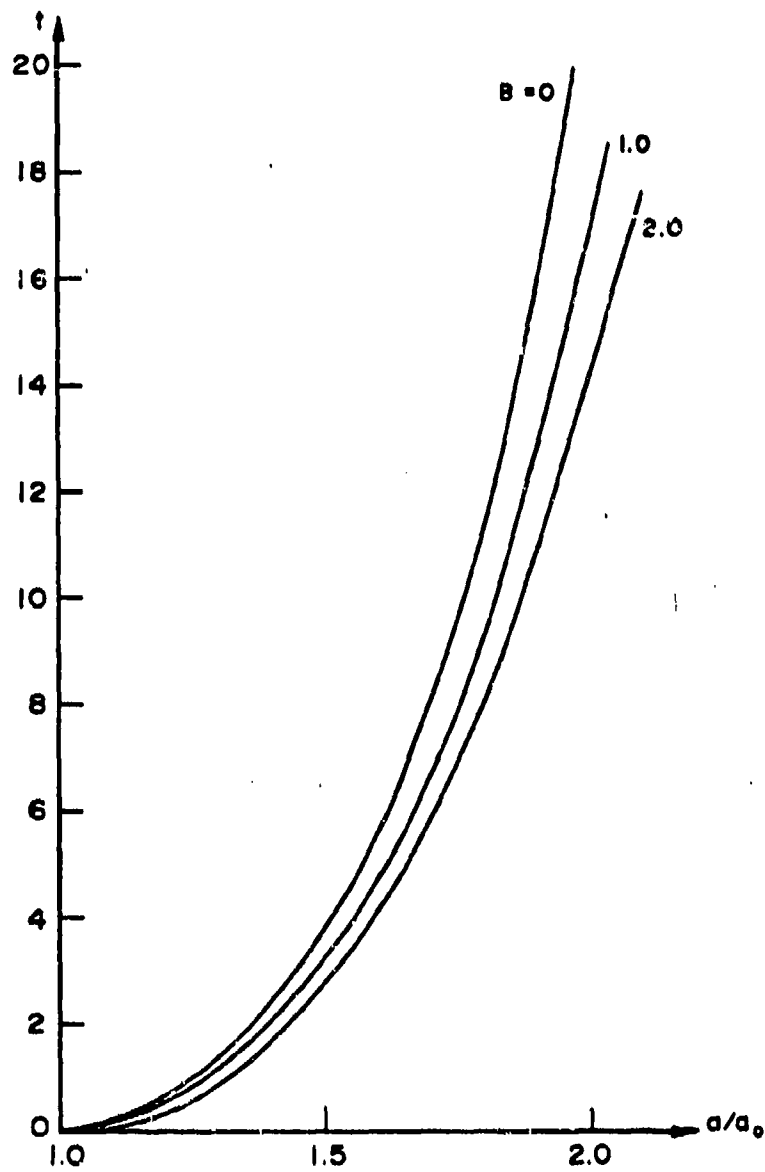


Figure 21: Two-dimensional drop, spreading rates for various  $B$   
with  $V = 1$ ,  $C = 1$ ,  $\epsilon = \lambda = 0$

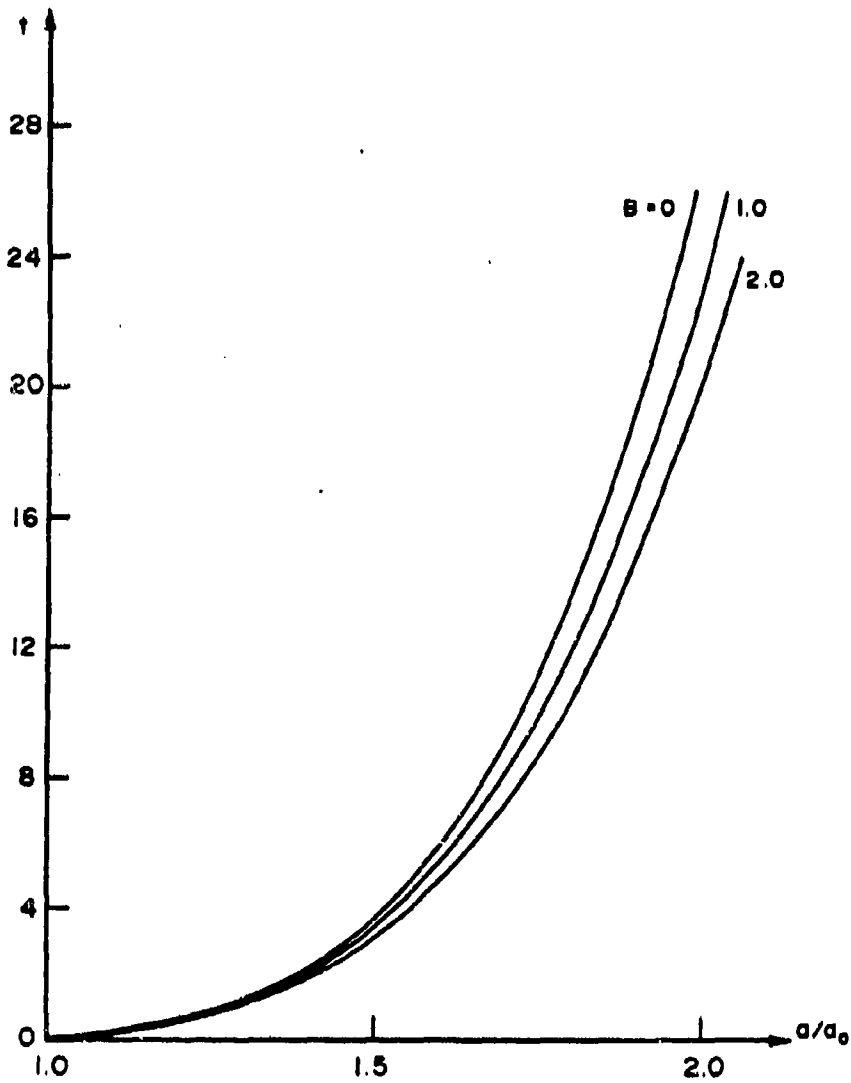


Figure 22: Axisymmetric drop, spreading rates for various  $B$  with  
 $V = C = 1, \epsilon = \lambda = 0$

translation. This accommodation takes place as follows. Initially, the rear contact angle is  $\theta_0^{\text{BACK}}$  and the forward contact angle is  $\theta_0^{\text{FRONT}}$ . If  $\theta_0^{\text{FRONT}} < \theta_A$  (advancing) angle) and  $\theta_0^{\text{BACK}} < \theta_R$  (receding angle) then both contact lines move. If, according to Figure 1, the corresponding contact-line speeds are equal, then the drop "slides" down the plane with constant shape. If, for example, the front contact line initially moves faster than the back one, the hydrodynamics causes the front angle to become more shallow slowing that contact line and the back angle to become more shallow speeding that contact line. The result tends toward the steady sliding case. Clearly, other cases also "rearrange" and approach the steady sliding case as long as  $\theta_R > 0$ .

The net result of these observations is that the component of gravity along the plate has only indirect effects on spreading characteristics since it merely adjusts the contact angles. The component of gravity normal to the plate directly affects spreading as discussed in Subsection 6.5.

## 7. CONCLUSIONS

The characteristics of Newtonian liquid drops spreading on smooth horizontal solid planes can be characterized by the non-dimensional groups  $V$  and  $C$  listed in Section 5. The intrinsic spreading and capillary effects are contained in the capillary number  $C$ ;  $C$  is large if the zero-shear-rate viscosity is large or the surface tension is small. The bulk features of the drop are contained in the volume  $V$ . The drop spreads more rapidly if  $C$  and  $V$  are increased.

The viscoelastic effects of the drop are characterized by the parameters  $\lambda$  and  $\epsilon$  listed in Section 5. Both  $\lambda$  and  $\epsilon$  measure the (single) relaxation time of the material though these are interpreted as stress relaxation and shear-thinning measures, respectively. For small contact angles

$\epsilon \gg \lambda$  so that shear thinning, if present, is much more important than stress relaxation.

We find that shear thinning is the dominant viscoelastic effect in thin drops. It has its greatest effects at small times (the drop begins spreading at  $t = 0$ ). For example shear thinning can accelerate the spreading rate by 50% after a few seconds if  $\epsilon = 5.0$ . However, there is a "catch-up" phenomenon that makes the spreading rate for long times very nearly that appropriate to the Newtonian drop having the same zero-shear-rate viscosity.

The main conclusion one draws from the present study is that the principal rheological property of interest in the spreading mechanics of drops on smooth surfaces is  $\mu_0$ , the zero-shear-rate viscosity. Thus for large ranges of material of interest to CSL, polymer additives greatly modify  $\mu_0$  and spreading is controlled by  $\mu_0$ .

The second most important rheological property is the variation  $\mu(\dot{\gamma})$  of shear viscosity with shear rate  $\dot{\gamma}$ . In the calculations presented we used the estimate  $\tau = 1$  sec for the maximum value of material relaxation time. Under most practical circumstances for CSL  $\epsilon \approx 0.01$  though it can in extreme cases get as large as  $\epsilon \approx 5.0$ . Even for  $\epsilon = 5.0$  we found rather modest acceleration in the spreading rate (compared to the case  $\epsilon = 0$  with the same  $\mu_0$ ); small values of  $\epsilon$  yield only minor accelerations. Hence, viscoelasticity affects spreading in a calculable way but its magnitude is seemingly small.

The effect of a vertical gravity on the spreading of a drop on a smooth horizontal plate is characterized by the Bond number  $B$  defined in Section 5. Vertical gravity distorts the shape of the liquid-air interface, steepens the contact angle and thus accelerates the spreading process. The effect is appreciable for large drops and negligible for small drops.

A drop on an inclined plane tilted an angle  $\beta$  to the horizontal has a component of gravity normal to the plate that affects spreading, as above, through a Bond number  $B \cos \beta$ . The component of gravity down the plate will result in the drop having steeper contact angles in front and shallower angles in the rear. The relations between these changes affect the spreading somewhat but principally lead to the drop moving bodily down the plate but not experiencing major changes in spreading rates.

Blank

## APPENDIX

1. Formulation
2. Lubrication Approximation
3. Evolution Equation
4. Solution Procedure

## 1. Formulation

We consider a drop of viscous liquid on a smooth rigid horizontal plane. We use a Cartesian coordinate system  $(x^*, y^*, z^*)$  for a two-dimensional drop, and a cylindrical polar coordinate system  $(r^*, \phi^*, z^*)$  for an axisymmetric drop. In both cases we take the rigid plane to coincide with the plane  $z^* = 0$ , with the  $z^*$  axis pointing vertically upwards.

In the case of a two-dimensional drop we consider the motion to be in the  $x^*, z^*$ -plane, with all quantities independent of  $y^*$ . Equations and relations pertaining to the two-dimensional case are designated by the letter P. For the axisymmetric drop all quantities are independent of the azimuthal coordinate  $\phi^*$ ; this case will be designated by the letter A.

### Initial State

In the two-dimensional case the initial-shape of the drop is taken to have the form

$$z^* = h_0^*(x^*) \quad , \quad -a_0 < x^* < a_0 \quad (1.1P)$$

with the end conditions

$$h_0^*(-a_0) = h_0^*(a_0) = 0 \quad . \quad (1.2P)$$

The initial contact angle  $\theta_0$  is given by

$$\tan \theta_0 = \frac{dh_0^*}{dx^*}(-a_0) = -\frac{dh_0^*}{dx^*}(a_0) \quad . \quad (1.3P)$$

The initial volume per unit length (in the  $y^*$  direction) is

$$V^* = \int_{-a_0}^{a_0} h_0^*(x^*) dx^* \quad . \quad (1.4P)$$

In the axisymmetric case the above initial data are replaced by

$$z^* = h_0^*(r^*) \quad , \quad 0 \leq r^* < a_0 \quad (1.1A)$$

with

$$h_0^*(a_0) = 0 \quad ; \quad (1.2A)$$

the contact angle  $\theta_0$  is given by

$$\tan \theta_0 = - \frac{dh_0^*}{dr^*}(a_0) \quad , \quad (1.3A)$$

and the volume is

$$V^* = 2\pi \int_0^{a_0} r^* h_0^*(r^*) dr^* \quad . \quad (1.4A)$$

### Drop Dynamics

At time  $t^* > 0$  we denote by  $a^*(t^*)$  the half-width of the drop in the two-dimensional case and its radius in the axisymmetric case. Thus we have the initial condition

$$a^*(0) = a_0 \quad . \quad (1.5)$$

We take the shape of the drop at time  $t^*$  to have the form

$$z^* = h^*(x^*, t^*) \quad , \quad -a^*(t^*) < x^* < a^*(t^*) \quad (1.6P)$$

with

$$h^*(-a^*(t^*), t^*) = h^*(a^*(t^*), t^*) = 0 \quad (1.7P)$$

in the two-dimensional case, and

$$z^* = h^*(r^*, t^*) \quad , \quad 0 \leq r^* < a^*(t^*) \quad (1.6A)$$

with

$$h^*(a^*(t^*), t^*) = 0 \quad (1.7A)$$

in the axisymmetric case. The contact angle at time  $t^*$  is denoted by

$\theta^* = \theta^*(t^*)$ , and is given by

$$\tan \theta^* = \frac{\partial h^*}{\partial x^*} (-a^*(t^*), t^*) = - \frac{\partial h^*}{\partial x^*} (a^*(t^*), t^*) \quad (1.8P)$$

or

$$\tan \theta^* = - \frac{\partial h^*}{\partial r^*} (a^*(t^*), t^*) \quad (1.8A)$$

respectively. Conservation of the volume of the drop over time gives the additional constraint

$$V^* = \int_{-a^*(t^*)}^{a^*(t^*)} h^*(x^*, t^*) dx^* \quad (1.9P)$$

or

$$V^* = 2\pi \int_0^{a^*(t^*)} r^* h^*(r^*, t^*) dr^* \quad (1.9A)$$

The rate of change of the quantity  $a^*$  at any instant  $t^*$  is taken, on empirical grounds, to be proportional to the difference between the angle  $\theta^*$  and the advancing contact angle  $\theta_A$ . The latter is the static equilibrium angle when the drop is on the point of spreading. The implied relation has the form

$$\frac{da^*}{dt^*} = \kappa (\theta^* - \theta_A) \quad (1.10)$$

where  $\kappa > 0$  is an empirically determined constant, and where  $\theta_A \geq 0$ .

#### Equations and Boundary Conditions

The motion is governed by the Navier-Stokes and continuity equations,

$$\rho \left( \frac{\partial \underline{v}^*}{\partial t^*} + \underline{v}^* \cdot \nabla^* \underline{v}^* \right) = - \nabla^* p^* + \nabla^* \cdot \underline{S}^* - \rho g \hat{z} \quad (1.11)$$

$$\nabla^* \cdot \underline{v}^* = 0 \quad (1.12)$$

where  $\rho$  is the density,  $\underline{v}^* = (u^*, 0, w^*)$  is the velocity vector,  $p^*$  is the pressure,  $\underline{S}^*$  is the extra-stress tensor,  $g$  is acceleration due to gravity,

and  $\hat{z}$  is unit vector in the upward vertical direction. A constitutive relation between the stress and the deformation-rate will be given below.

The boundary conditions are:

(i) The normal velocity component is zero on the rigid plane,

$$w^* = 0 \quad \text{on} \quad z^* = 0 \quad ; \quad (1.13)$$

(ii) As explained by Dussan V. and Davis [1], the usual no-slip condition at the rigid boundary needs to be modified to avoid the appearance of a singularity at the contact line. Following Greenspan [2] we take the condition to be

$$(\gamma^{*2}/\mu_0) S_{13}^* = h^* u^* \quad \text{on} \quad z^* = 0 \quad (1.14)$$

where  $\mu_0$  is the zero-shear-rate viscosity,  $\gamma^*$  is a slip length (distance from the contact line over which slip takes place) and  $S_{13}^*$  represents the  $x^* z^*$ -component of extra stress in the two-dimensional case, and the  $r^* z^*$ -component in the axisymmetric case.

(iii) The kinematic condition at the free surface is

$$w^* = \frac{\partial h^*}{\partial t^*} + u^* \frac{\partial h^*}{\partial x^*} \quad \text{on} \quad z^* = h^*(x^*, t^*) \quad (1.15P)$$

or

$$w^* = \frac{\partial h^*}{\partial t^*} + u^* \frac{\partial h^*}{\partial r^*} \quad \text{on} \quad z^* = h^*(r^*, t^*) \quad (1.15A)$$

(iv) The dynamic boundary condition at the free surface is

$$- [p^*] \underline{n} + \underline{S}^* \cdot \underline{n} = 2H^* \sigma \underline{n} \quad \text{on} \quad z^* = h^* \quad (1.16)$$

where  $[p^*]$  denotes the pressure difference across the interface,  $\sigma$  is the

surface tension,  $\underline{n}$  is the outward unit normal to the surface, and  $2H^*$  is the mean curvature of the interface.

### Rheology

A constitutive equation that is suitable for polymer solutions is the generalized Maxwell model,

$$\underline{S}^* + \tau \left\{ \frac{\partial \underline{S}^*}{\partial t^*} + (\underline{v}^* \cdot \nabla^*) \underline{S}^* + \frac{1}{2} (\underline{\omega}^* \cdot \underline{S}^* - \underline{S}^* \cdot \underline{\omega}^*) - \frac{1}{2} \beta (\underline{S}^* \cdot \dot{\underline{Y}}^* + \dot{\underline{Y}}^* \cdot \underline{S}^*) \right\} = \mu \dot{\underline{Y}}^* \quad (1.17)$$

where

$$\dot{\underline{Y}}^* = \nabla^* \underline{v}^* + (\nabla^* \underline{v}^*)^T \quad (1.18)$$

$$\underline{\omega}^* = \nabla^* \underline{v}^* - (\nabla^* \underline{v}^*)^T \quad (1.19)$$

$\tau$  is the relaxation time of the liquid and  $\beta$  is a number, which in practical situations can range between  $-1$  and  $+1$ . (See, for example, Petrie [3].) Rather than analyze the whole range of values of  $\beta$ , we shall consider only two special cases, namely  $\beta = 0$  and  $\beta = 1$ . When  $\beta = 0$  the model (1.17) reduces to the well-known corotational Maxwell model. In steady unidirectional shear flow this model yields shear thinning and both first and second normal stress differences, and yields stress relaxation in unsteady simple shear. When  $\beta = 1$ , (1.17) reduces to the upper convected Maxwell model. Here there is no shear thinning in simple shear, the viscosity remaining constant at its zero-shear-rate value, but first and second normal stress differences, as well as stress relaxation, are present. By studying these two models we have the possibility of assessing the various rheological effects on spreading; in particular the differences between the  $\beta = 0$  and  $\beta = 1$  case will distinguish the influence of shear thinning.

## 2. Lubrication Approximation

We proceed on the basis of the assumption that the initial angle  $\theta_0$  is very small. This enables us to use the lubrication approximation, in which all quantities are appropriately scaled, and then the equations and boundary conditions are expanded in powers of  $\theta_0$ . The first-order problem is what is retained in the limit  $\theta_0 \rightarrow 0$ .

A dimensionless time  $t$  is defined by

$$t = t^* \sigma \theta_0^3 / a_0 \mu_0 \quad (2.1)$$

and dimensionless coordinates  $(x, z)$  in the two-dimensional problem, and  $(r, z)$  in the axisymmetric problem, are defined by

$$x = x^* / a_0, \quad z = z^* / (a_0 \theta_0), \quad r = r^* / a_0. \quad (2.2)$$

The dimensionless shape of the drop becomes  $h(x, t)$  or  $h(r, z)$  respectively, where

$$h = h^* / (a_0 \theta_0). \quad (2.3)$$

The half-width (radius) of the drop is  $a(t)$ , given by

$$a(t) = a^*(t^*) / a_0 \quad (2.4)$$

and the contact angle is

$$\theta(t) = \theta^*(t^*) / \theta_0 \quad (2.5)$$

with the final equilibrium (advancing) contact angle given by

$$\theta_F = \theta_A / \theta_0. \quad (2.6)$$

We also define a dimensionless volume by

$$V = V^* / a_0^2 \theta_0 \quad (2.7P)$$

or

$$V = V^* / a_0^3 \theta_0. \quad (2.7A)$$

Dimensionless velocity components (u,w) and pressure p are given by

$$u = u^*/(\kappa\theta_0) \quad , \quad w = w^*/(\kappa\theta_0^2) \quad , \quad p = p^*(a_0\theta_0/\mu_0\kappa) \quad . \quad (2.8)$$

Finally we have a dimensionless stress tensor  $\underline{s}$  defined by

$$\underline{s} = \underline{s}^*(a_0/\mu_0\kappa) \quad . \quad (2.9)$$

### Initial State

Note that our non-dimensionalization gives that the drop has unit half-width (radius) initially, and the initial contact angle  $\theta(0)$  is also unity.

In the two-dimensional case the initial shape has the form

$$z = h_0(x) \quad , \quad -1 < x < 1 \quad (2.10P)$$

with the end conditions

$$h_0(-1) = h_0(1) = 0 \quad . \quad (2.11P)$$

Using the lubrication approximation  $\theta_0 \rightarrow 0$  we find the condition for the initial contact angle to be

$$\frac{dh_0}{dx}(-1) = -\frac{dh_0}{dx}(1) = 1 \quad . \quad (2.12P)$$

We also have the volume condition

$$v = \int_{-1}^1 h_0(x) dx \quad . \quad (2.13P)$$

The analogous expressions in the axisymmetric case are

$$z = h_0(r) \quad , \quad 0 \leq r < 1 \quad (2.10A)$$

with

$$h_0(1) = 0 \quad , \quad (2.11A)$$

at the contact line

$$\frac{dh_0}{dr}(1) = -1 \quad , \quad (2.12A)$$

and

$$V = 2\pi \int_0^1 rh(r)dr \quad . \quad (2.13A)$$

### Drop Dynamics

The shape of the drop at time  $t$  in the two-dimensional case is

$$z = h(x,t) \quad , \quad -a(t) < x < a(t) \quad (2.14P)$$

with

$$h(-a(t),t) = h(a(t),t) = 0 \quad (2.15P)$$

while in the axisymmetric case it is

$$z = h(r,t) \quad , \quad 0 \leq r < a(t) \quad (2.14A)$$

with

$$h(a(t),t) = 0 \quad . \quad (2.15A)$$

In the lubrication approximation the contact angle  $\theta(t)$  is given by

$$\theta(t) = h_x(-a(t),t) = -h_x(a(t),t) \quad (2.16P)$$

or

$$\theta(t) = -h_r(a(t),t) \quad . \quad (2.16A)$$

The volume conservation condition (1.9) becomes

$$V = \int_{-a(t)}^{a(t)} h(x,t) dx \quad (2.17P)$$

or

$$V = 2\pi \int_0^{a(t)} rh(r,t) dr \quad (2.17A)$$

Equations (1.10) and (2.16) combine to give the following differential equation for the dynamics of the drop:

$$\frac{da(t)}{dt} = C[-h_x(a(t),t) - \theta_F] \quad (2.18P)$$

or

$$\frac{da(t)}{dt} = C[-h_r(a(t),t) - \theta_F] \quad (2.18A)$$

where  $C$  is the capillary defined by

$$C = \frac{\mu_0^k}{\sigma\theta_0^2} \quad (2.19)$$

Equation (2.18) is subject to the initial conditions

$$a(0) = 1 \quad (2.20)$$

#### Equations and Boundary Conditions

In the lubrication limit  $\theta_0 \rightarrow 0$  the Navier-Stokes and continuity equations in the two-dimensional case reduce to

$$-p_x + S_{13,z} = 0 \quad (2.21P)$$

$$-p_z - B/C = 0 \quad (2.22P)$$

$$u_x + w_z = 0 \quad (2.23P)$$

where  $S_{13}$  is the  $x,z$  component of the stress tensor, and where  $B$  is the Bond number defined by

$$B = \frac{\rho g a^2}{\sigma} \quad (2.24)$$

Note that  $S_{13}$ , which is associated with shear thinning in viscoelastic materials, is the only stress component that remains in the reduced system (2.21)-(2.23). Components such as  $S_{11}$ ,  $S_{22}$ ,  $S_{33}$ , associated with normal stress differences, are not explicitly present in the equation of motion in the lubrication limit.

The corresponding equations in the axisymmetric case are

$$-p_r + S_{13,z} = 0 \quad (2.21A)$$

$$-p_z - B/C = 0 \quad (2.22A)$$

$$(ru)_r + (rw)_z = 0 \quad (2.23A)$$

The boundary conditions are:

- (i) zero normal velocity at the rigid plane

$$w = 0 \quad \text{on} \quad z = 0 \quad (2.25)$$

- (ii) modified slip condition at the rigid plane

$$\gamma^2 S_{13} = hu \quad \text{on} \quad z = 0 \quad (2.26)$$

where

$$\gamma^2 = (\gamma^*/a_0 \theta_0)^2 \quad (2.27)$$

- (iii) kinematic interfacial condition

$$h_t + C(uh_x - w) = 0 \quad \text{on} \quad z = h(x,t) \quad (2.28P)$$

or

$$h_t + C(uh_r - w) = 0 \quad \text{on} \quad z = h(r,t) \quad (2.28A)$$

(iv) dynamic boundary conditions on the interface are

$$h_{xx} + Cp = 0 \quad \text{on} \quad z = h(x,t) \quad (2.29p)$$

or

$$h_{rr} + \frac{1}{r} h_r + Cp = 0 \quad \text{on} \quad z = h(r,t) \quad (2.29A)$$

and

$$S_{13} = 0 \quad \text{on} \quad z = h \quad (2.30)$$

### Rheology

Using the scalings indicated above we find that the constitutive relation (1.17) becomes, in dimensionless form,

$$\underline{\underline{S}} + \lambda \frac{\partial \underline{\underline{S}}}{\partial t} + \epsilon C \left\{ (\underline{\underline{v}} \cdot \nabla) \underline{\underline{S}} + \frac{1}{2} (\underline{\underline{\omega}} \cdot \underline{\underline{S}} - \underline{\underline{S}} \cdot \underline{\underline{\omega}}) - \frac{1}{2} \beta (\underline{\underline{S}} \cdot \dot{\underline{\underline{Y}}} + \dot{\underline{\underline{Y}}} \cdot \underline{\underline{S}}) \right\} = \dot{\underline{\underline{Y}}} \quad (2.31)$$

where in the lubrication approximation

$$\dot{\underline{\underline{Y}}} = \begin{pmatrix} 0 & u_z \\ u_z & 0 \end{pmatrix}, \quad \underline{\underline{\omega}} = \begin{pmatrix} 0 & -u_z \\ u_z & 0 \end{pmatrix} \quad (2.32)$$

and where  $\lambda$ ,  $\epsilon$  are relaxation parameters defined by

$$\lambda = \frac{\tau \sigma \theta_0^3}{a_0 \mu_0}, \quad (2.33)$$

$$\epsilon = \frac{\tau \sigma \theta_0^2}{a_0 \mu_0}. \quad (2.34)$$

Note that

$$\lambda/\epsilon = \theta_0. \quad (2.35)$$

The form of (2.31) shows that  $\lambda$  is a measure of stress relaxation while  $\epsilon$  is a measure of shear thinning. Hence (2.35) implies that stress relaxation only becomes important when shear thinning is absent.

The components of equation (2.31) are

$$S_{11} + \lambda \frac{\partial S_{11}}{\partial t} + \epsilon C \left\{ -u_z S_{13} - \beta u_z S_{13} \right\} = 0 \quad (2.36)$$

$$S_{13} + \lambda \frac{\partial S_{13}}{\partial t} + \frac{1}{2} \epsilon C \left\{ u_z (S_{11} - S_{33}) - \beta u_z (S_{11} + S_{33}) \right\} = u_z \quad (2.37)$$

$$S_{33} + \lambda \frac{\partial S_{33}}{\partial t} + \epsilon C \left\{ u_z S_{13} - \beta u_z S_{13} \right\} = 0 \quad (2.38)$$

When  $\beta = 1$  (upper convected Maxwell model) we obtain  $S_{33} = 0$  from (2.38) and then (2.37) reduces to

$$S_{13} + \lambda \frac{\partial S_{13}}{\partial t} = u_z \quad (2.39)$$

In this model only stress relaxation is relevant, and there is no shear thinning.

When  $\beta = 0$  (corotational Maxwell model) we neglect  $\lambda$  by virtue of (2.35) and the system (2.36)-(2.38) reduces to

$$S_{11} - \epsilon C u_z S_{13} = 0 \quad (2.40)$$

$$S_{13} + \frac{1}{2} \epsilon C u_z (S_{11} - S_{33}) = u_z \quad (2.41)$$

$$S_{33} + \epsilon C u_z S_{13} = 0 \quad (2.42)$$

From these we obtain

$$S_{13} = \frac{u_z}{1 + \epsilon^2 C^2 u_z^2} \quad (2.43)$$

which implies that the effective viscosity for simple shear is

$$\frac{1}{1 + \epsilon^2 C^2 u_z^2} \quad (2.44)$$

### 3. EVOLUTION EQUATION

In the two-dimensional case we integrate (2.23) and use the boundary conditions (2.25) and (2.28) to obtain the equation

$$\frac{\partial h}{\partial t} + c \frac{\partial}{\partial x} (hQ) = 0 \quad (3.1P)$$

where

$$hQ = \int_0^{h(x,t)} u(x,z,t) dz \quad (3.2P)$$

From integration of (2.22P) we obtain

$$p = \bar{p}(x,t) - Bz/C \quad (3.3P)$$

so that the boundary condition (2.29P) gives

$$h_{xx} + C\bar{p}(x,t) - Bh = 0 \quad (3.4P)$$

Substituting into (2.21P), we obtain

$$h_{xxxx} - Bh_x + CS_{13,z} = 0 \quad (3.5P)$$

Integrating this with respect to  $z$  and using (2.30) we obtain

$$CS_{13} = (h_{xxx} - Bh_x)(h-z) \quad (3.6P)$$

An analogous procedure for the axisymmetric case leads to the analog of equation (3.1P), namely

$$\frac{\partial h}{\partial t} + \frac{c}{r} \frac{\partial}{\partial r} \int_0^{h(r,t)} ru(r,z,t) dz = 0 \quad (3.1A)$$

while the analog of (3.5P) is found to be

$$\frac{\partial}{\partial r} (h_{rr} + \frac{1}{r} h_r - Bh) + CS_{13,z} = 0 \quad (3.5A)$$

Integration of this gives

$$CS_{13} = (h-z) \frac{\partial}{\partial r} (h_{rr} + \frac{1}{r} h_r - Bh) \quad (3.6A)$$

The next steps depend on which of the constitutive relations ( $\beta = 0$  or  $\beta = 1$ ) is being used.

Upper Convected Maxwell Model ( $\beta = 1$ )

We substitute (3.6F) into the constitutive relation (2.39) to obtain

$$C_{u_z} = (Gh)(h-z) + \lambda \frac{\partial}{\partial t} \{ (Gh)(h-z) \} \quad (3.7F)$$

where

$$Gh \equiv h_{xxxx} - Bh_x \quad (3.8F)$$

Integrating (3.7) with respect to  $z$  and using the boundary condition (2.26) we obtain

$$C_u = (Gh)(\gamma^2 + hz - \frac{1}{2} z^2) + \lambda \frac{\partial}{\partial t} \{ (Gh)(hz - \frac{1}{2} z^2) \} \quad (3.9F)$$

We integrate again with respect to  $z$  over 0 to  $h$ . This gives, in the notation of (3.2F),

$$ChQ = (Gh)(\gamma^2 h + \frac{1}{3} h^3) + \frac{\lambda}{12} [(Gh)h^3]_t + \frac{\lambda}{4} h^2 [(Gh)h]_t \quad (3.10F)$$

We now substitute this into (3.1F), which becomes

$$h_t + \frac{\partial}{\partial x} \left\{ (Gh)(\gamma^2 h + \frac{1}{3} h^3) + \frac{\lambda}{12} [(Gh)h^3]_t + \frac{\lambda}{4} h^2 [(Gh)h]_t \right\} = 0 \quad (3.11F)$$

This is to be solved subject to the initial condition

$$h(x,0) = h_0(x) \quad (3.12F)$$

the boundary conditions (2.15F) and the constraint (2.17F). In addition we assume that  $h_0(x)$  and  $h(x,t)$  are symmetric about  $x = 0$ .

The axisymmetric analog of (3.7F) is

$$C_{u_z} = (Dh)(h-z) + \lambda \frac{\partial}{\partial t} \{ (Dh)(h-z) \} \quad (3.7A)$$

where

$$Dh = \frac{\partial}{\partial r} (h_{rr} + \frac{1}{r} h_r - Bh) \quad (3.8A)$$

After two integrations and application of the boundary condition (2.26)

we obtain

$$c \int_0^{h(r,t)} r u dz = r(Dh) \left( \gamma^2 h + \frac{1}{3} h^3 \right) + \frac{\lambda}{12} r [(Dh)h^3]_t + \frac{\lambda}{4} r h^2 [(Dh)h]_t \quad (3.10A)$$

and then (3.1A) becomes

$$h_t + \frac{1}{r} \frac{\partial}{\partial r} \left\{ r(Dh) \left( \gamma^2 h + \frac{1}{3} h^3 \right) + \frac{\lambda}{12} r [(Dh)h^3]_t + \frac{\lambda}{4} r h^2 [(Dh)h]_t \right\} = 0 \quad (3.11A)$$

The initial condition is

$$h(r,0) = h_0(r) \quad (3.12A)$$

and we have the boundary condition (2.15A) and the constraint (2.17A).

We assume also the symmetry condition

$$\frac{dh_0}{dr}(0) = \frac{\partial h}{\partial r}(0,t) = 0 \quad (3.13A)$$

#### Corotational Maxwell Model ( $\beta = 0$ )

We combine (3.6P) and (2.43) to obtain

$$\frac{Cu_z}{1 + \varepsilon^2 C^2 u_z^2} = (Gh)(h-z) = F \quad , \quad \text{say} \quad (3.14P)$$

from which we deduce that

$$Cu_z = \frac{1 - \sqrt{1 - 4\varepsilon^2 F^2}}{2\varepsilon^2 F} \quad (3.15P)$$

As is usual in flows with shear thinning a solution ceases to exist if  $\varepsilon$  is too large. We assume  $\varepsilon$  to be sufficiently small that an expansion of (3.15) is possible, whereupon we obtain

$$Cu_z = (Gh)(h-z) + \varepsilon^2 [(Gh)(h-z)]^3 + O(\varepsilon^4) \quad (3.16P)$$

Integrating and using the boundary condition (2.26) we obtain

$$Cu = (Gh) \left\{ \gamma^2 + \frac{1}{2} h^2 - \frac{1}{2} (h-z)^2 \right\} + \frac{1}{4} \epsilon^2 (Gh)^3 \left\{ h^4 - (h-z)^4 \right\}. \quad (3.17P)$$

Integrating again over 0 to h, we obtain

$$ChQ = (Gh) \left( \gamma^2 h + \frac{1}{3} h^3 \right) + \frac{1}{5} \epsilon^2 (Gh)^3 h^5. \quad (3.18P)$$

Substituting into (3.1P) we now obtain

$$h_{tt} + \frac{\partial}{\partial x} \left\{ (Gh) \left( \gamma^2 h + \frac{1}{3} h^3 \right) + \frac{1}{5} \epsilon^2 (Gh)^3 h^5 \right\} = 0. \quad (3.19P)$$

For the axisymmetric case an exactly analogous procedure leads to the equation

$$h_{tt} + \frac{1}{r} \frac{\partial}{\partial r} \left\{ r(Dh) \left( \gamma^2 h + \frac{1}{3} h^3 \right) + \frac{1}{5} \epsilon^2 r(Dh)^3 h^5 \right\} = 0 \quad (3.19A)$$

with conditions (3.12A) and (3.13A).

It is convenient to transform to a moving frame in which the position of the contact line is fixed. We set

$$\xi = x/a(t) \quad (3.20P)$$

in the two-dimensional case, and

$$\xi = r/a(t) \quad (3.20A)$$

in the axisymmetric case. In both cases the interfacial shape is given by

$$z = h(\xi, t) \quad (3.21)$$

defined on

$$-1 < \xi < 1 \quad (3.22P)$$

or

$$0 \leq \xi < 1 \quad (3.22A)$$

respectively.

For the motion of the drop the equations (2.18) and (2.20) become

$$\frac{da}{dt}(t) = C [-h_{\xi}(1,t)/a(t) - \theta_F] \quad (3.23)$$

with

$$a(0) = 1 \quad (3.24)$$

The various forms of the evolution equation are transformed as follows:

Equation (3.11P) becomes

$$\mathcal{L}h + \frac{1}{a} \frac{\partial}{\partial \xi} \left\{ (\hat{G}h) (\gamma^2 h + \frac{1}{3} h^3) + \frac{\lambda}{12} \mathcal{L}[(\hat{G}h)h^3] + \frac{\lambda}{4} h^2 \mathcal{L}[(\hat{G}h)h] \right\} = 0 \quad (3.25P)$$

where

$$\mathcal{L} \equiv \frac{\partial}{\partial t} - b(t)\xi \frac{\partial}{\partial \xi} \quad (3.26)$$

$$b(t) = \frac{d}{dt} \ln a(t) \quad (3.27)$$

$$\hat{G}h = h_{\xi\xi\xi} - Ba^2 h_{\xi} \quad (3.28P)$$

Similarly equation (3.11A) becomes

$$\mathcal{L}h + \frac{1}{a} \frac{\partial}{\partial \xi} \left\{ \xi (\hat{D}h) (\gamma^2 h + \frac{1}{3} h^3) + \frac{\lambda \xi}{12} \mathcal{L}[(\hat{D}h)h^3] + \frac{\lambda \xi}{4} h^2 \mathcal{L}[(\hat{D}h)h] \right\} = 0 \quad (3.25A)$$

where

$$\hat{D}h = \frac{\partial}{\partial \xi} \left\{ h_{\xi\xi} + \frac{1}{\xi} h_{\xi} - Ba^2 h \right\} \quad (3.28A)$$

Equation (3.19P) for the corotational model becomes

$$\mathcal{L}h + \frac{1}{a} \frac{\partial}{\partial \xi} \left\{ (\hat{G}h) (\gamma^2 h + \frac{1}{3} h^3) + \frac{\xi^2}{5a^6} (\hat{G}h)^3 h^5 \right\} = 0 \quad (3.29P)$$

while (3.19A) becomes

$$\mathcal{L}h + \frac{1}{a} \frac{\partial}{\partial \xi} \left\{ \xi (\hat{D}h) (\gamma^2 h + \frac{1}{3} h^3) + \frac{\xi^2}{5a^6} \xi (\hat{D}h)^3 h^5 \right\} = 0 \quad (3.29A)$$

The initial conditions are

$$h(\xi, 0) = h_0(\xi) \quad (3.30)$$

where

$$h_0(\xi) = h_0(x) \quad , \quad -1 < x < 1 \quad (3.31P)$$

or

$$h_0(\xi) = h_0(r) \quad , \quad 0 \leq r < 1 \quad (3.31A)$$

and the constraints (2.11)-(2.13) apply to the initial shape. The boundary conditions (2.15) become

$$h(-1, t) = h(1, t) = 0 \quad (3.32P)$$

or

$$h(1, t) = 0 \quad (3.32A)$$

The volume conservation condition (2.17) becomes

$$\frac{V}{a(t)} = \int_{-1}^1 h(\xi, t) d\xi \quad (3.33P)$$

in the two-dimensional case, and

$$\frac{V}{a^2(t)} = 2\pi \int_0^1 \xi h(\xi, t) d\xi \quad (3.33A)$$

in the axisymmetric case. We impose also symmetry conditions at  $\xi = 0$ .

#### 4. SOLUTION PROCEDURE

The problem posed in the previous Section is solved by transforming the evolution equation (3.11) or (3.19) into a system of ordinary differential equations in the time  $t$ . This is done by use of the Galerkin method.

In the two-dimensional case we define functions

$$h_n(\xi) = \begin{cases} (1 - \xi^2)^n, & n = 0, 1, 2, \dots \\ 0, & n < 0 \end{cases} \quad (4.1)$$

for integer values of  $n$ . Correspondingly we define

$$\alpha_n = \int_{-1}^1 h_n(\xi) d\xi, \quad n \geq 0 \quad (4.2P)$$

These are then given by

$$\alpha_0 = 2, \quad \alpha_n = \frac{2n}{2n+1} \alpha_{n-1}, \quad n \geq 1 \quad (4.3P)$$

Next we introduce the Galerkin expansion

$$h(\xi, t) = \sum_{k=1}^{N+1} \phi_k(t) h_k(\xi) \quad (4.4)$$

where the  $\phi_k$  are unknown functions of  $t$ . We refer to (4.4) as an N-term Galerkin expansion, since one of the  $\phi$ 's, namely  $\phi_{N+1}$ , is fixed in terms of  $\phi_1, \dots, \phi_N$  through the volume conservation condition (3.33). In fact, substituting (4.4) into (3.33P) we obtain

$$\alpha_{N+1} \phi_{N+1}(t) = v/a(t) - \sum_{k=1}^N \alpha_k \phi_k(t) \quad (4.5P)$$

All the boundary conditions and constraints on  $h$  are satisfied by the representation (4.4)-(4.5).

With the aid of (4.4) we construct a system of  $N + 2$  ordinary differential equations for the functions  $\phi_1(t), \dots, \phi_{N+1}(t), a(t)$ . First we have that (3.23)-(3.24) become

$$\dot{a} = c [2\phi_1/a - \theta_F] \quad (4.6)$$

with

$$a(0) = 1 \quad (4.7)$$

Next we have from differentiation of (4.5) the equation

$$\alpha_{N+1} \dot{\phi}_{N+1} + \sum_{k=1}^N \alpha_k \dot{\phi}_k + \frac{Vb}{a} = 0 \quad (4.8P)$$

where  $b$  is defined by (3.27). Then we substitute (4.4) into the appropriate evolution equation, multiply by  $h_n(\xi)$  for  $n = 1, 2, \dots, N$  and integrate over  $(-1, +1)$  with respect to  $\xi$ . In the case of the upper convected Maxwell model evolution equation (3.25P) this gives the following system of  $N$  ordinary differential equations:

$$a^4 \left\langle h_n \mathcal{L}h \right\rangle + \left\langle h_n \frac{\partial}{\partial \xi} \left\{ (\hat{G}h) \left( \gamma^2 h + \frac{1}{3} h^3 \right) + \frac{\lambda}{12} \mathcal{L}[(\hat{G}h)h^3] + \frac{1}{4} h^2 \mathcal{L}[(\hat{G}h)h] \right\} \right\rangle = 0 \quad (4.9P)$$

$n = 1, 2, \dots, N$ , where  $\langle \cdot \rangle$  denotes the inner product

$$\left\langle h_n f \right\rangle = \int_{-1}^1 h_n(\xi) f(\xi) d\xi \quad (4.10)$$

We now have  $N + 2$  equations, namely (4.6), (4.8P) and (4.9P); they are evidently highly nonlinear. The condition (2.12P) on the initial slope gives the initial condition

$$\phi_1(0) = \frac{1}{2} \quad (4.11)$$

The fact that we wish to allow for the drop to have arbitrary initial shape is expressed through the initial data

$$\phi_2(0), \dots, \phi_N(0) \text{ arbitrary} \quad (4.12)$$

Finally we have from (4.5P) that

$$\alpha_{N+1} \phi_{N+1}(0) = V - \sum_{k=1}^N \alpha_k \phi_k(0) \quad (4.13P)$$

Thus we have a total of  $N + 2$  initial conditions: (4.7), (4.11), (4.12) and (4.13P).

In the case of the corotational Maxwell model (3.29P) we follow the same procedure and obtain in place of (4.9P) the system

$$a^4 \langle h_n \dot{c}_h \rangle + \langle h_n \frac{\partial}{\partial \xi} \left\{ (\hat{G}h) (\gamma^2 h + \frac{1}{3} h^3) + \frac{\epsilon^2}{5a^6} (\hat{G}h)^3 h^5 \right\} \rangle = 0, \quad n = 1, \dots, N. \quad (4.14P)$$

The other equations and the initial conditions are as before.

In the axisymmetric case we again use the system of basic functions (4.1). We also define

$$\beta_n = \int_0^1 \xi h_n(\xi) d\xi, \quad n \geq 0 \quad (4.2A)$$

which gives

$$\beta_n = \frac{1}{2(n+1)}, \quad n \geq 0 \quad (4.3A)$$

The Galerkin expansion (4.4) is again used. The volume constraint (3.33) now takes the form

$$\beta_{N+1} \phi_{N+1}(t) = \frac{V}{2\pi a^2(t)} - \sum_{k=1}^N \beta_k \phi_k(t) \quad (4.5A)$$

Equation (4.6) and the accompanying condition (4.7) remain applicable.

In place of (4.8P) we differentiate (4.5A) to obtain

$$\beta_{N+1} \dot{\phi}_{N+1} + \sum_{k=1}^N \beta_k \dot{\phi}_k + \frac{Vb}{\pi a^2} = 0 \quad (4.8A)$$

The evolution equation (3.25A), after integration, becomes

$$a^4 \left\langle \xi h_n \mathcal{L}h \right\rangle + \left\langle h_n \frac{\partial}{\partial \xi} \left\{ \xi (\hat{D}h) (\gamma^2 h + \frac{1}{3} h^3) + \frac{\lambda \xi}{12} \mathcal{L}[(\hat{D}h)h^3] + \frac{\lambda \xi}{4} h^2 \mathcal{L}[(\hat{D}h)h] \right\} \right\rangle = 0, \quad n = 1, \dots, N \quad (4.9A)$$

where the inner product is defined by (4.10). The evolution equation (3.29A) becomes

$$a^4 \left\langle \xi h_n \mathcal{L}h \right\rangle + \left\langle h_n \frac{\partial}{\partial \xi} \left\{ \xi (\hat{D}h) (\gamma^2 h + \frac{1}{3} h^3) + \frac{\epsilon^2 \xi}{5a^6} (\hat{D}h)^3 h^5 \right\} \right\rangle = 0$$

$$n = 1, \dots, N \quad (4.14A)$$

The initial conditions (4.7), (4.11) and (4.12) continue to apply, while (4.13P) is replaced by

$$\beta_{N+1} \phi_{N+1}(0) = \frac{v}{2\pi} - \sum_{k=1}^N \beta_k \phi_k(0) \quad (4.13A)$$

The respective systems are solved numerically using a modified standard package called DGEAR.

## REFERENCES

1. Dussan, V., E. B. and Davis, S. H. J. Fluid Mech., 65 71, 1974.
2. Greenspan, H. P. J. Fluid Mech., 84, 125, 1978.
3. Petrie, C. J. S. "Elongational flows". Pitman 1979